DRSAR/SA/R-23

DESCRIPTION OF LASER SPOT MOTION DURING DESIGNATION OF MOVING TARGETS

GEORGE J. SCHLENKER

JUNE 1977

US ARMY ARMAMENT MATERIEL READINESS COMMAND
SYSTEMS ANALYSIS DIRECTORATE
ROCK ISLAND, ILLINOIS 61201

DISPOSITION

Destory this report when nc longer needed. Do not return it to the originator.

DISCLAIMER

The findings in this report are not to be construed as an official Department of the Army position.

WARNING

Information and data contained in this document are based on input available at the time of preparation. Because the results may be subject to change, this document should not be construed to represent the official position of the US Army Development & Readiness Command unless so stated.

UNCLASSIFIED

SECURITY CLASSIFICATION OF THIS PAGE *(When Data Entered)*

REPORT DOCUMENTATION PAGE		READ INSTRUCTIONS BEFORE COMPLETING FORM
1. REPORT NUMBER DRSAR/SA/R-23	2. GOVT ACCESSION NO.	3. RECIPIENT'S CATALOG NUMBER
4. TITLE *(and Subtitle)* DESCRIPTION OF LASER SPOT MOTION DURING DESIGNATION OF MOVING TARGETS		5. TYPE OF REPORT & PERIOD COVERED Report - Final 6. PERFORMING ORG. REPORT NUMBER
7. AUTHOR(s) George J. Schlenker		8. CONTRACT OR GRANT NUMBER(s)
9. PERFORMING ORGANIZATION NAME AND ADDRESS US Army Armament Materiel Readiness Command Systems Analysis Directorate (DRSAR-SA) Rock Island, IL 61201		10. PROGRAM ELEMENT, PROJECT, TASK AREA & WORK UNIT NUMBERS
11. CONTROLLING OFFICE NAME AND ADDRESS US Army Armament Materiel Readiness Command Systems Analysis Directorate (DRSAR-SA) Rock Island, IL 61201		12. REPORT DATE June 1977 13. NUMBER OF PAGES 91
14. MONITORING AGENCY NAME & ADDRESS*(if different from Controlling Office)*		15. SECURITY CLASS. *(of this report)* UNCLASSIFIED 15a. DECLASSIFICATION/DOWNGRADING SCHEDULE

16. DISTRIBUTION STATEMENT *(of this Report)*

Approved for public release; distribution unlimited.

17. DISTRIBUTION STATEMENT *(of the abstract entered in Block 20, if different from Report)*

18. SUPPLEMENTARY NOTES

19. KEY WORDS *(Continue on reverse side if necessary and identify by block number)*

Stochastic Processes	Laser Spot Jitter
Digital Filters	Laser Signatures
Digital Simulation	Atmospheric Scintillation
Tracking Error	Guided Projectiles

20. ABSTRACT *(Continue on reverse side if necessary and identify by block number)*

This report identifies and discusses two distinct dynamic components in a mathematical model of the stochastic motion of a laser spot on a moving target as viewed from the position of the designator. One of these components is contributed by manual tracking and possesses approximately second-order dynamics. The other component is contributed jointly by laser device and atmospheric propagation effects (scintillation) and exhibits nearly first-order dynamics.

(continued)

DD FORM 1 JAN 73 1473 EDITION OF 1 NOV 65 IS OBSOLETE

UNCLASSIFIED

SECURITY CLASSIFICATION OF THIS PAGE *(When Data Entered)*

20. Abstract (continued).

Both frequency-domain and time-domain analyses are pursued in comparing the mathematical model with a sample of spot motion test data. Algorithms for digital implementation of the components of the stochastic model are derived. The implementation is conceived as an input generator for a laser target signature model. There is an exposition of certain distortions which are produced in the autospectra of the stochastic components due to the implementation. Additionally, some statistical aspects of parameter estimation are presented.

CONTENTS

Page

LIST OF TABLES

LIST OF FIGURES

LIST OF SYMBOLS

Symbol	Definition
σ_t	standard deviation of the tracking error component of laser spot motion (m)
σ_s	standard deviation of the scintillation error component of laser spot motion (m)
ν	natural frequency (hz)
ν_t	natural corner (cutoff) frequency of the second-order tracking error process (hz)
ν_s	natural cutoff frequency of the first-order scintillation error process (hz)
ω	angular frequency (rad sec^{-1}). When subscripted with t and s, the symbol denotes the respective angular corner frequencies for the tracking and scintillation processes.
$H_t^2(\nu)$	squared modulus of the transfer function for the tracking error. In Chapter 1 this symbol is also used for the tracking error component of the autospectrum of spot motion (m^2/hz).
$H_s^2(\nu)$	squared modulus of the transfer function for the scintillation error. In Chapter 1 this symbol is also used for the scintillation error component of the autospectrum of spot motion (m^2/hz).
$H^2(\nu)$	autospectrum of the (analog) spot motion process (m^2/hz)
$[H'(\omega)]^2$	autospectrum of a stochastic process expressed in terms of the angular frequency (m^2/(rad/sec))
A	gain constant in the expression for the autospectrum of the tracking error process (m^2/hz)
B	gain constant in the expression for the autospectrum of the scintillation error process (m^2/hz)
$\Gamma_{xx}(\nu)$	autospectrum of the azimuthal component of the spot motion process (m^2/hz)

Symbol	Definition
$\Gamma_{yy}(\nu)$	autospectrum of the elevation component of the spot motion process (m^2/hz)
$\Gamma'_{xx}(\omega)$	azimuthal autospectrum expressed in terms of the angular frequency (m^2/(rad/sec))
$\gamma_{xx}(t)$	autocovariance of the azimuthal component of laser spot motion (m^2), (Chapter 2) and of a stochastic process $\{x(t)\}$, (Chapters 3 and 4)
$\rho_{xx}(t)$	autocorrelation of the azimuthal component of laser spot motion
s	Laplace transform variable
$H'(s)$	transfer function of a first-order process (Chapter 3)
$\bar{H}(s)$	transfer function of a first-order process normalized to produce unity gain for s=0.
$H_z(z)$	digital transfer function for a first-order dynamic process (Chapter 3) and a second-order dynamic process (Chapter 4)
x_t	the value of a stochastic time series at a discrete point t
n_t	the value of a digital white noise process at a discrete point t
σ_n^2	variance of the white-noise input to a digital filter
$\Gamma_{nn}(\nu)$	autospectrum of the white-noise input to a digital filter
$\gamma_{nn}(t)$	autocovariance function for white noise
T	sampling (generation) time interval for generating a digital stochastic process $\{x_t\}$
$E[\ ]$	expected value operator for ensemble averages
a	warped and normalized analog cutoff frequency for a first-order process (Chapter 3)
ω_a	warped and normalized analog cutoff frequency for a second-order process (Chapter 4)

Symbol	Definition
$H_1^2(\nu)$	squared modulus of the first-order digital error process
$H_2^2(\nu)$	squared modulus of the second-order digital error process
T^*	time interval for sampling an analog error process or subsampling a digital error process
$F(s)$	Laplace transform of a general, dynamic process (Chapter 5)
$F^*(s)$	Laplace transform of a time-sampled general dynamic process (Chapter 5)
ν_f	the Nyquist or folding frequency of a time-sampled process
ω_n	the n th angular harmonic of the folding frequency
m	order of subsampling (Chapter 5)
$w(t)$	weight function or lag window used in computing a smoothed autospectrum. This function is subscripted to refer to particular types.
$\hat{\gamma}(t)$	the autocovariance function estimated from a particular sample time series
$\hat{\Gamma}_{xx}(\omega)$	the estimated and smoothed autospectrum of the process $\{x(t)\}$
λ_k	the k th spectral moment of an analog stochastic process (Chapter 6)
$\tilde{\lambda}_k$	the k th spectral moment of a digital stochastic process
$\bar{\lambda}_k$	the k th normalized spectral moment of a digital stochastic process (Chapter 6)

Next page is blank.

INTRODUCTION

Background

In estimating guidance error dispersion of laser guided projectiles, one quickly comes to recognize the importance of laser spot motion as a primary external error source. Over a period of several years the author and his colleagues have been involved in making such estimates for the Copperhead (CLGP) projectile and its predecessors. In this connection I have frequently emphasized the importance of this error source and its significance for the guidance accuracy of several flight vehicles. References [1]* and [2] illustrate this emphasis. As a consequence of the importance attached to laser spot motion and related aspects of the laser signature such as pulse dropout and laser spillover, considerable efforts have been spent studying tracking error for various designators and trackers. Some analytic models of the tracking error are given in References [3] and [4]. In particular, Reference [4] describes the statistical techniques used to produce an analytic model descriptive of the tracking error of the Ground Laser Locator Designator (GLLD) observed during the CLGP OT-1 Tracking Tests. Each of the above models are descriptive of the performance of a particular combination of tracking device and tracker operator faced with a particular tracking problem.

---

* Square-bracketed numbers refer to cited literature.

[1] Memorandum for Record, AMSAR-SAM, 23 July 1975, subject: Army-Navy Guided Projectile Effectiveness Study.

[2] Schlenker, G. J. and Heider, R. D., Distribution of Angle of Obliquity of Laser-Guided Projectiles With Respect to the Target at Impact, DRSAR/SA/N-51, (AD A032683), US Army Armament Command, Rock Island, IL, August 1976.

[3] Pastrick, H. L. and Hollman, H. C., Analysis and Digital Simulation Models for CLGP: Martin Marietta Aerospace Design, Report No. RG-75-29, (Appendix G, Pulse Dropout and Pulse Dither Subroutines), US Army Missile Command, Huntsville, AL, Dec 1974.

[4] Letter, AMSAR-SA, 10 Dec 74, subject: Reduction and Analysis of CLGP-OT-1 Tracking Data.

Particular models of this type are statistical summaries suitable for a digital computer simulation of the process of spot motion as seen by the designator, which can be used as input to terminal guidance simulations and laser target reflectance models.*

An accurate characterization of laser spot motion, whatever its source, is also important because (stochastic) process dynamics are also pertinent to the problem of laser spillover and its consequence for guidance accuracy. In Reference [5], which addresses this problem, spot motion was treated as a second-order stochastic process.

In an effort to standardize laser designator testing procedures, increased attention (Reference [6]) has been given to various phenomena which give rise to laser spot motion: device jitter, atmospheric propagation effects (scintillation and beam steering), and designator tracking error. In a field-test environment, these phenomena all contribute and cannot be isolated by direct measurement. Consequently, some of the past analyses, which have considered "spot motion" and "tracking error" as interchangeable terms, have been somewhat indiscriminate. Pragmatically this lack of attention to the components of spot motion may not have been of great significance in that the joint process is what is of concern in guided projectile accuracy analysis. However, a closer attention to the components of spot motion does produce clarity in understanding the disparate phenomena.

---

* In studies done at ARMCOM the laser signatures seen by the projectile seeker are generated by a laser target reflectance model using a T55 tank as the target. Validation of this model is contained in the following report: Beard, J., Rice, D., and Ladd, D., Target Reflection Illumination Model With Second Order (TRIMS), (CONF), ERIM Report No. 192200-2-F, Environmental Research Institute of Michigan, Aug 1975. Updated documentation of this type of model will be included in a report in preparation: Ladd, D., A Multifaceted Target Signature Model With Digital Imaging.

[5] Schlenker, G. J., "Proportion of Energy Spilled Over a Target During Tracking With a Laser Designator and Implications for Terminal Guidance," Systems Analysis Directorate Activities Summary November 1976, Report No. DRSAR/SA/N-60, US Army Armament Command, Rock Island, IL, December 1976.

[6] Minutes of a Meeting at White Sands Missile Range, NM, STEWS-TE-AG, 18 June 1976, subject: Uniform Standards for Laser Designator Developments.

Overview of the Report

This report reexamines some of the spot motion data from the CLGP OT-1 Tracking Tests with the intention of identifying and statistically isolating the stochastic component attributable to human tracking error from those produced by other mechanisms. For notational convenience thruout the balance of this report, device jitter and beam-steering effects due to the atmosphere will be subsummed by the term "scintillation component." This simplification is considered justifiable because of the dominance of atmospheric effects in the example treated here. In decomposing laser spot motion into tracking (t) and scintillation (s) components, one exploits the fact that these components have different dynamics which are nearly separable in the frequency domain.

Much of this report is devoted to deriving mathematical expressions useful in characterizing the stochastic spot motion process and in producing digital implementations for simulation purposes. Mathematical results are generally presented in maximum generality with other applications in mind. Numerical examples are provided thruout the report to give the reader a (hopefully) better sense of magnitude. For convenience of exposition, the report is divided into the following six chapters:

Chapter 1. Decomposition of Laser Spot Motion into Tracking and Scintillation components.

Chapter 2. The Analytical Autocovariance Function for Laser Spot Motion Developed From the Spectral Density.

Chapter 3. Digital Computer Implementation for the First-Order Component of the Spot Motion Error.

Chapter 4. Digital Computer Implementation for the Second-Order Component of the Spot Motion Error.

Chapter 5. Autospectra of the Digital Error Processes.

Chapter 6. Spectral Moments and Parameter Estimation.

Computer source program listings for pertinent methods are presented in the Appendicies.

Summary

In Chapter 1 it is argued that the autospectrum of spot motion consists mainly of separable, additive components: one due to the human tracking

process, possessing approximately second-order dynamics, and the other due to processes having approximately first-order dynamics with a significantly higher crossover frequency than the human tracker component. Expressions for the gain constant in each component of the autospectrum are developed in terms of the variance of each component. A numerical example of the analytic autospectrum is compared with an experimental estimate derived from the azimuthal error of Run 75A of the CLGP OT-1 Tracking Tests. Parameter values of the analytic model were selected by trial and error, under constraints, to produce an acceptable Chebychev fit to the experimental autospectrum in the sense of minimizing the maximum residual.

It is sometimes useful to make comparisons between analytic models and experimental estimates in the time domain as well as in the frequency domain. Altho time- and frequency-domain descriptions are equivalent, autocorrelations are often more intuitively appealing. For example, the time interval which must separate two time series segments before they are effectively uncorrelated can be observed immediately. Chapter 2 develops an expression for the autocovariance (and autocorrelation) function for the spot motion process and extends the example of Chapter 1 by comparing the autocorrelation function of the analytic model with an experimental estimate.

Chapter 3 treats the digital implementation of the first-order component of spot motion. Implementation is achieved by low-pass filtering of gaussian white noise. Expressions are developed for the coefficients of the digital filter and for the variance of the input noise required to produce a given output process variance.

Chapter 4 parallels the developments in Chapter 3 while treating the second-order component of the spot motion process. This development is the basis of the principal algorithm* which the ARMCOM Systems Analysis Directorate and others have used to describe laser spot motion during the past four years. An updated version of the computer program which we use to describe spot motion is found in Appendix A.

---

* A special case of this algorithm is presented in subroutine DITH of Reference [3].

Chapter 5 develops the autospectra of the scintillation (first-order) and tracking (second-order) dynamic components as implemented digitally. The autospectrum of each component is separately compared with its continuous-time (analog) counterpart. Some sources of distortion in the digital implementation and in the process of making statistical estimates of autospectra are identified and are quantified using the first-order process as an example. These results suggest the means to minimize spectral distortions.

Chapter 6 derives expressions for the spectral moments of each of the stochastic components of the spot motion process. Additionally, statistical estimators are derived for the parameters of pure first-order and Butterworth second-order processes which exploit the spectral moments.

Next page is blank.

CHAPTER 1

DECOMPOSITION OF LASER SPOT MOTION INTO TRACKING AND SCINTILLATION COMPONENTS

Let the variance of the spot motion at the target due to only tracker error be σ_t^2 in (m^2). Experience with the TOW and GLLD trackers as well as airborne man-operated trackers shows that tracking error exhibits approximately second-order dynamics.

Let the tracking process be second-order Butterworth so that the spectral density is given by

$$H_t^2(\nu) = \frac{A}{1 + (\nu/\nu_t)^4} \quad , \; 0 \leq \nu < \infty \; , \tag{1.1}$$

with gain constant A and natural corner frequency ν_t.

The variance or total power of the process is

$$\sigma_t^2 = \int_0^\infty H_t^2(\nu)\, d\nu \tag{1.2}$$

$$= A\, \nu_t \int_0^\infty \frac{df}{1 + f^4} \tag{1.3}$$

$$\sigma_t^2 = A\, \nu_t\, \pi \sqrt{2} / 4 \quad . \tag{1.4}$$

Whence

$$A = \frac{4\, \sigma_t^2}{\sqrt{2}\, \pi\, \nu_t} \tag{1.5}$$

$$A = \frac{2 \sqrt{2}\, \sigma_t^2}{\pi\, \nu_t} \quad . \qquad (m^2/hz)$$

Normally, the corner frequency ν_t is determined by the dynamics of the human motor system and lies below one hertz.

Scintillation data* suggest that the majority of scintillation power lies above one hertz at frequencies to which the human cannot respond. Consequently, tracking error noise and scintillation noise are substantially uncorrelated. Data on intensity of scintillation above 10 hertz suggest this process has nearly first-order dynamics.

We suppose that a first-order process, uncorrelated with the tracking process, with variance σ_s^2 is superposed thereon. The spectrum for this scintillation process is given by

$$H_s^2(\nu) = \frac{B}{1 + (\nu/\nu_s)^2} \quad , \tag{1.6}$$

with corner frequency ν_s.

Therefore,

$$\sigma_s^2 = \int_0^\infty H_s^2(\nu)\, d\nu \tag{1.7}$$

$$\sigma_s^2 = B\nu_s \int_0^\infty \frac{df}{1 + f^2} \tag{1.8}$$

$$\sigma_s^2 = B\,\nu_s\,\frac{\pi}{2} \quad . \tag{1.9}$$

Whence,

$$B = \frac{2}{\pi}\,\frac{\sigma_s^2}{\nu_s} \qquad (m^2/hz). \tag{1.10}$$

*Some power spectra for percent modulation are given on pp 224 of [7], Wolfe, W. L. (Ed) Handbook of Military Infrared Technology, Office of Naval Research, Wash D.C., c. 1965.

If the processes are superposed, the spectrum of the joint process is just the sum of the component spectra. Letting the joint autospectrum be $H^2(\nu)$,*

$$H^2(\nu) = H_t^2(\nu) + H_s^2(\nu) \tag{1.11}$$

$$H^2(\nu) = \frac{A}{1 + (\nu/\nu_t)^4} + \frac{B}{1 + (\nu/\nu_s)^2} \quad . \tag{1.12}$$

Example

Based on daytime tracking tests at WSMR during the CLGP OT 1 Tests, the following parameter values were selected from Run 75A for the azimuthal error:

$\nu_t = 0.7$ hz , $\nu_s = 3$ hz

$\sigma_t = 0.230$ m , $\sigma_s = 0.165$ m (at 3 km range)

$A = 6.8038\ 10^{-2}$, $B = 5.7773\ 10^{-3}$ (m^2/hz).

Numerical results are shown in Table 1 and in Figure 1.

TABLE 1. ANALYTIC ESTIMATES OF THE TRACKING AND SCINTILLATION COMPONENTS OF AZIMUTHAL LASER SPOT MOTION IN THE AUTOSPECTRUM

ν	$H_t^2(\nu)$	$H_s^2(\nu)$	$H^2(\nu)$ (m^2/hz)
0.3	$6.582\ 10^{-2}$	$5.720\ 10^{-3}$	$7.154\ 10^{-2}$
0.5	$5.398\ 10^{-2}$	$5.621\ 10^{-3}$	$5.961\ 10^{-2}$
0.7	$3.402\ 10^{-2}$	$5.479\ 10^{-3}$	$3.950\ 10^{-2}$
1.0	$1.317\ 10^{-2}$	$5.200\ 10^{-3}$	$1.837\ 10^{-2}$
1.5	$3.081\ 10^{-3}$	$4.622\ 10^{-3}$	$7.702\ 10^{-3}$
2.0	$1.006\ 10^{-3}$	$4.000\ 10^{-3}$	$5.005\ 10^{-3}$
4.0	$6.375\ 10^{-5}$	$2.080\ 10^{-3}$	$2.144\ 10^{-3}$

*An alternative notation for the spectral density (autospectrum) is $\Gamma_{xx}(\nu)$, for azimuth, and $\Gamma_{yy}(\nu)$, for elevation.

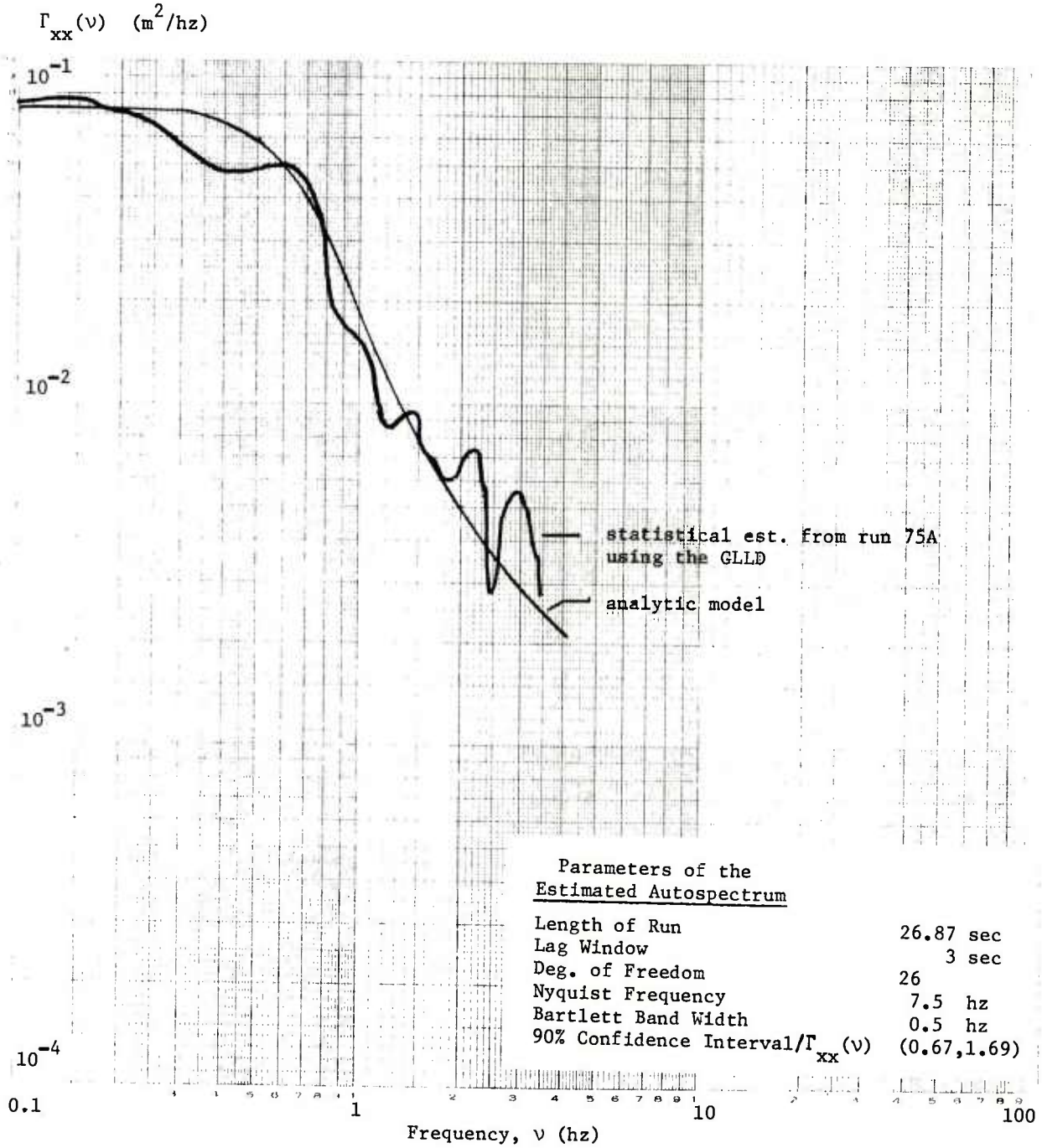

Figure 1. Comparison of an Analytic Model of the Autospectrum of Azimuthal Laser Spot Motion With an Experimental Estimate

CHAPTER 2

THE ANALYTICAL AUTOCOVARIANCE FUNCTION FOR LASER SPOT MOTION DEVELOPED FROM THE SPECTRAL DENSITY

The spectral density (autospectrum) of laser spot motion in, say, the x-direction due to the joint effects of tracking jitter and atmospheric scintillation (beam steering) is given by

$$\Gamma_{xx}(\nu) = \frac{A}{1+(\nu/\nu_t)^4} + \frac{B}{1+(\nu/\nu_s)^2}, \quad 0 \leq \nu < \infty, \tag{2.1}$$

where

$$A = \frac{2\sqrt{2}\ \sigma_t^2}{\pi\ \nu_t}$$

$$B = \frac{2\ \sigma_s^2}{\pi\ \nu_s},$$

with variance contributed by tracking σ_t^2 and variance contributed by scintillation σ_s^2. By definition,

$$\sigma_t^2 + \sigma_s^2 = \int_0^\infty \Gamma_{xx}(\nu)\, d\nu. \tag{2.2}$$

The natural corner frequency of the second-order tracking process is ν_t and that of the first-order scintillation process is ν_s.

An alternative expression for (2.1) in terms of the angular frequency ω is $\Gamma'_{xx}(\omega)$.

$$\Gamma'_{xx}(\omega) = \Gamma_{xx}(\nu(\omega))\left|\frac{d\nu}{d\omega}\right|$$

or

$$\Gamma'_{xx}(\omega) = \frac{1}{2\pi}\,\Gamma_{xx}\left(\frac{\omega}{2\pi}\right) \tag{2.3}$$

$$\Gamma'_{xx}(\omega) = \frac{A\,\omega_t^4\,(2\pi)^{-1}}{\omega_t^4 + \omega^4} + \frac{B\,\omega_s^2\,(2\pi)^{-1}}{\omega_s^2 + \omega^2} \quad . \tag{2.4}$$

Now, the spectral density is by definition the Fourier cosine transform of the autocovariance function $\gamma_{xx}(t)$.

$$\Gamma'_{xx}(\omega) = \frac{2}{\pi}\int_0^\infty \gamma_{xx}(t)\cos\omega t\,dt \ . \tag{2.5}$$

In general, the Fourier transform pairs $f(t)$ and $g(\omega)$ are related by:

$$g(\omega) = \int_0^\infty f(t)\cos(\omega t)\,dt$$

$$f(t) = 2\pi\int_0^\infty g(\omega)\cos(\omega t)\,d\omega \ . \tag{2.6}$$

From (2.5),

$$\gamma_{xx}(t) = \pi^2\int_0^\infty \Gamma'_{xx}(\omega)\cos(\omega t)\,d\omega \ . \tag{2.7}$$

The following general results will be used to develop an expression for $\gamma_{xx}(t)$ for the spot motion process:

$$\int_0^\infty (a_1^2 + \omega^2)^{-1}\cos\omega t\,d\omega = (2\pi a_1)^{-1} e^{-a_1 t} \tag{2.8}$$

$$\int_0^\infty (a_2^4 + \omega^4)^{-1}\cos\omega t\,d\omega =$$

$$(2\pi)^{-1} a_2^{-3} e^{-a_2 t/\sqrt{2}} \sin\left(\frac{\pi}{4} + \frac{a_2 t}{\sqrt{2}}\right) \quad . \tag{2.9}$$

Using the expression for $\Gamma'_{xx}(\omega)$ in (2.4),

$$\int_0^\infty \Gamma'_{xx}(\omega) \cos \omega t \, d\omega = B \nu_s (2\pi)^{-1} e^{-\omega_s t}$$

$$+ A \nu_t (2\pi)^{-1} e^{-\omega_t t/\sqrt{2}} \sin\left(\frac{\pi}{4} + \frac{\omega_t t}{\sqrt{2}}\right) . \qquad (2.10)$$

With A and B as defined in (2,1) and with (2.7),

$$\gamma_{xx}(t) = \sqrt{2}\, \sigma_t^2 \, e^{-\omega_t t/\sqrt{2}} \sin\left(\frac{\pi}{4} + \frac{\omega_t t}{\sqrt{2}}\right) + \sigma_s^2 \, e^{-\omega_s t} . \qquad (2.11)$$

The autocorrelation function is defined as

$$\rho_{xx}(t) = \gamma_{xx}(t)/\gamma_{xx}(0) . \qquad (2.12)$$

In this case,

$$\gamma_{xx}(0) = \sigma_t^2 + \sigma_s^2 . \qquad (2,13)$$

Example

Using parameter estimates from tracking run number 75A of the CLGP OT 1 Tracking Tests,

$\nu_t = 0.7$ hz $\qquad \omega_t = 4.398$ r/s

$\nu_s = 3$ hz $\qquad \omega_s = 18.850$ r/s

$\sigma_t = 0.23$ m $\qquad$ (at 3 km range)

$\sigma_s = 0.165$ m

$\sigma_t^2 / (\sigma_t^2 + \sigma_s^2) = 0.6586$

$\sigma_s^2 / (\sigma_t^2 + \sigma_s^2) = 0.3414$

$$\rho_{xx}(t) = 0.9314 \exp(-3.11t) \sin(0.7854 + 3.11t) + 0.3414 \exp(-18.85t). \qquad (2.14)$$

This result is compared with the experimental estimates in Figure 2.

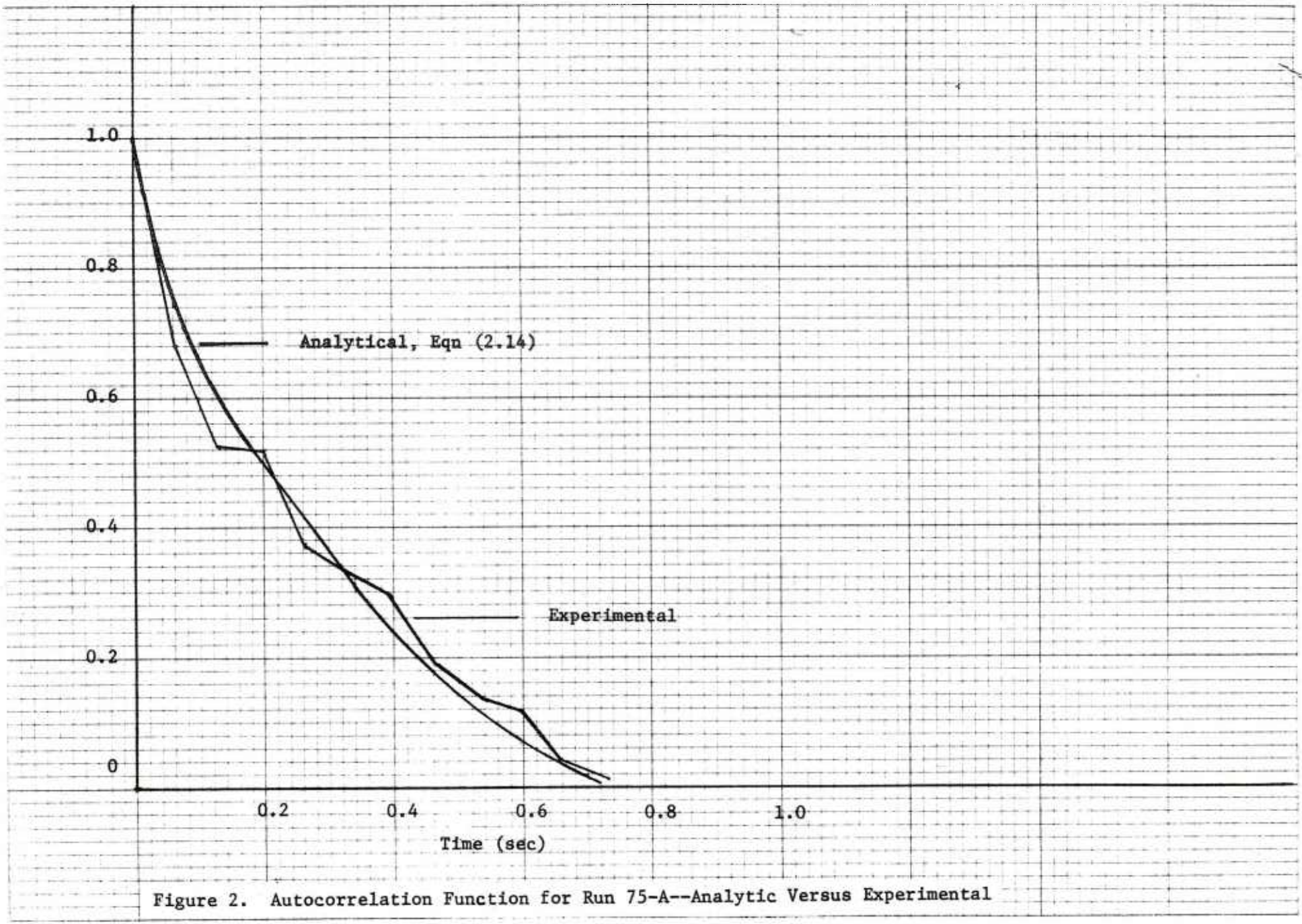

Figure 2. Autocorrelation Function for Run 75-A--Analytic Versus Experimental

Next page is blank.

CHAPTER 3

DIGITAL COMPUTER IMPLEMENTATION FOR THE FIRST-ORDER COMPONENT OF THE SPOT MOTION ERROR

Marginal statistics for the first-order process are assumed gaussian. However, for brevity the word "gaussian" is often omitted in describing the process. One implements a first-order, continuous (or, analog) stochastic process with a first-order digital filter having a discrete, mean-zero gaussian white noise input. The design of the filter is based upon the assumption that the continuous-time process is being time sampled.

Continuous-time (Analog) Processes

The following first-order transfer function H'(s):

$$H'(s) = \frac{(B/2\pi)^{1/2}\ \omega_s}{s + \omega_s} \tag{3.1}$$

having a continuous, white noise input generates the autospectrum

$$[H'(\omega)]^2 = \frac{(B/2\pi)\ \omega_s^2}{\omega^2 + \omega_s^2} \quad , \tag{3.2}$$

as in equation (2.4) of Chapter 2, where the autospectrum of the output is just the squared modulus:

$$[H'(\omega)]^2 = H'(j\omega)\ H'(-j\omega) \tag{3.3}$$

for a white noise input of unit variance.

For convenience a normalized version of (3.1) is employed such that gain is unity for s equal to zero:

$$\overline{H}(s) = \omega_s/(s + \omega_s) \quad . \tag{3.4}$$

Attention to the variance of the input white noise is deferred until later.

Filter Design

A time sampling of the continuous process characterized by (3.4) can be used as the basis of the digital implementation. The z-transform describing the digital implementation of (3.4) can be obtained by performing a bilinear transformation from the s-plane into the z-plane. (See Walsh [8] or Stanley [9]). The bilinear z-transform is taken by substituting

$$s = (z - 1)/(z + 1) \tag{3.5}$$

into (3.4).

To minimize distortion of the spectrum of the digital process relative to the equivalent analog process, we use a warped analog cutoff frequency, a (instead of ω_s), where

$$a = \tan(\omega_s T/2) = \tan(\pi \nu_s T),^* \tag{3.6}$$

with sampling interval T and desired angular cutoff frequency ω_s or natural cutoff frequency ν_s.

Using the warped cutoff frequency, the digital transfer function** is

$$H_z(z) = \frac{a}{\frac{z - 1}{z + 1} + a} \quad . \tag{3.7}$$

---

*This is a normalized version of the warping transformation of frequency required by the bilinear transformation. Normalization is achieved by division by 2/T.

**The digital transfer function is the ratio of the z-transforms of output to input of a digital filter.

[8] Walsh, P. J., A Study of Digital Filters, AD710381, Naval Postgraduate School, Monterey, CA., Dec 1969.
[9] Stanley, W. D. Digital Signal Processing, Reston Pub. Co., Inc., Reston, VA., c. 1975.

The useful (cannonical) form of (3.7) is, after manipulation,

$$H_z(z) = \frac{a_o(1 + z^{-1})}{1 + bz^{-1}} \quad , \tag{3.8a}$$

with

$$a_o = a/(a + 1)$$

$$b = (a - 1)/(a + 1). \tag{3.8b}$$

Remembering that z^{-1} is the backspace operator, implementation of the desired digital filter follows directly from (3.8). Notationally, let the noise input to the filter at time index t be n_t and the output at t be x_t, with t integer.

Then,

$$x_t + bx_{t-1} = a_o n_t + a_o n_{t-1} \tag{3.9}$$

or

$$x_t = a_o n_t + a_o n_{t-1} - bx_{t-1} \cdot \tag{3.10}$$

Since the desired output spectrum requires a white noise input,

$$E[n_t n_{t-k}] = 0 \quad , k \neq 0 \tag{3.11}$$

$$= \sigma_n^2 \quad , k = 0.$$

Ratio of Output to Input Variances

In selecting the value of noise variance of the input to yield a particular output variance, it is necessary to know the ratio of output to input variance of the filter. In the following development an expression for this ratio will be derived. It will be useful to employ the following

notation for the covariance function:

$$\gamma_{xx}(k) = E[x_t x_{t-k}]. \tag{3.12}$$

In this notation, we desire

$$\gamma_{xx}(0)/\sigma_n^2 \text{ or } \gamma_{xx}(0)/\gamma_{nn}(0).$$

Taking the mathematical expectation of the product of n_t with both sides of (3.10) yields

$$E[x_t n_t] = a_o \sigma_n^2 \quad , \text{ (t integer)}, \tag{3.13}$$

since

$$E[n_t n_{t-1}] = 0$$

and

$$E[n_t x_{t-1}] = 0 \ .$$

Similarly, taking the expectation of the product of n_{t-1} with both sides of (3.10) yields

$$E[x_t n_{t-1}] = a_o(1 - b)\ \sigma_n^2 \quad . \tag{3.14}$$

After squaring both sides of (3.10) and taking the mathematical expectation,

$$\gamma_{xx}(0) = E[x_t^2] = E[a_o^2\, n_t^2 + 2\, a_o^2\, n_t n_{t-1} - 2\, a_o b n_t x_{t-1} - 2\, a_o b n_{t-1} x_{t-1}$$
$$+ a_o^2\, n_{t-1}^2 + b^2 x_{t-1}^2] \quad . \tag{3.15}$$

With (3.13) and (3.14),

$$\gamma_{xx}(0)/\gamma_{nn}(0) = 2\, a_o^2/(1 + b). \tag{3.16}$$

Alternatively, with (3.8b) ,

$$\gamma_{xx}(0)/\gamma_{nn}(0) = a/(a + 1) \ . \tag{3.17}$$

This is the desired result.

Summary

In summary, to simulate a first-order, mean-zero process x_t having a desired cutoff frequency ν_s and standard deviation σ_s, one can employ the digital filter given by (3.10) with a gaussian, white noise input n_t having standard deviation given by

$$\sigma_n = [\gamma_{nn}(0)/\gamma_{xx}(0)]^{1/2}\sigma_s$$

$$\sigma_n = [(a + 1)/a]^{1/2}\sigma_s \ , \tag{3.18}$$

with a given by (3.6) and filter constants given by (3.8b).

Next page is blank.

CHAPTER 4

DIGITAL COMPUTER IMPLEMENTATION FOR THE SECOND-ORDER COMPONENT OF THE SPOT MOTION ERROR

Analysis of a variety of man-operated trackers, such as those reported in [3], indicates that the marginal probability distribution function for the tracking component of laser spot motion is adequately described as gaussian. Additional experience with tracking records of this type indicates that a second-order dynamical system characterizes the tracking error. For most human trackers a good digital simulation of the mean-zero portion of the tracking error is obtained by filtering gaussian white noise with a second-order, low-pass Butterworth filter. As in Chapter 3, the design of the digital filter is based upon the assumption that the continuous-time (analog) process is being time sampled.

Continuous-time (Analog) Processes

The following transfer function describes a second-order analog process with analog corner frequency ω_a and damping constant ζ:

$$H_t(s) = \frac{\omega_a^2}{s^2 + 2\zeta\,\omega_a s + \omega_a^2} \quad . \tag{4.1}$$

Specifically for low-pass Butterworth filters $\zeta = 1/\sqrt{2}$ and

$$H_t(s) = \frac{\omega_a^2}{s^2 + \sqrt{2}\,\omega_a s + \omega_a^2} \quad . \tag{4.2}$$

The digital transfer function* associated with (4.2) is created by mapping from the s-plane into the z-plane using the bilinear z-transform.

*The digital transfer function is the ratio of the z-transforms of output to input sequences of a digital filter.

(See Walsh, P. J., Op Cit [8]). The bilinear z-transform is taken by substituting

$$s = (z - 1)/(z + 1) \tag{4.3}$$

in (4.2). Thus,

$$H_z(z) = H_t\left(\frac{z - 1}{z + 1}\right)$$

$$H_z(z) = \frac{\omega_a^2 (z + 1)^2}{(z - 1)^2 + \sqrt{2}\,\omega_a (z - 1)(z + 1) + \omega_a^2 (z + 1)^2} \quad . \tag{4.4}$$

Reduction of $H_z(z)$ to the form

$$\frac{a_o + a_1 z^{-1} + a_2 z^{-2}}{1 + b_1 z^{-1} + b_2 z^{-2}} \tag{4.5}$$

implies the digital filter, since z^{-1} is equivalent to a unit backspace operator. The coefficients in (4.5) are given by

$$a_o = a_2 = \omega_a^2/D$$

$$a_1 = 2\,a_o$$

$$b_1 = 2(\omega_a^2 - 1)/D$$

$$b_2 = (\omega_a^2 - \sqrt{2}\,\omega_a + 1)/D$$

with

$$D = \omega_a^2 + \sqrt{2}\,\omega_a + 1 \quad . \tag{4.6}$$

Notationally, let the noise input to the filter at time index t be n_t and the output at t be x_t, with t an integer. Then, from (4.5),

$$x_t + b_1 x_{t-1} + b_2 x_{t-2} = a_o n_t + a_1 n_{t-1} + a_2 n_{t-2} \quad . \tag{4.7}$$

Since the analog angular frequency ω_a associated with the bilinear transformation is "warped" or distorted relative to the desired digital cutoff angular frequency ω_t, we employ the relationship between these parameters:

$$\omega_a = \tan(\omega_t T/2)$$

or

$$\omega_a = \tan(\pi \nu_t T), \tag{4.8}$$

where T is the sampling period.

Parenthetically, note that a change in the sampling period, for a fixed digital cutoff frequency, would change ω_a and, by (4.6), would change the coefficients of the digital filter.

In operation, the filter arithmetic is performed as follows:

$$x_t = a_o n_t + a_1 n_{t-1} + a_2 n_{t-2} - b_1 x_{t-1} - b_2 x_{t-2} , \tag{4.9}$$

with t = 3, 4, ...

The filter is initialized by assigning $x_1 = x_2 = 0$, their mean values; and, then, cycling through a sufficient set of inputs to remove the effect of the initialization transient.

The form of (4.9) is referred to in the statistical literature, e.g., [10] and [11]*, as a mixed autoregressive, moving average model since the output x_t depends upon past values of the output -- x_{t-1} and x_{t-2} -- as

*[10] Box, G. E. P. and Jenkins, G. M., Time Series Analysis: Forecasting and Control, Holden-Day, San Francisco, c. 1970.

[11] Jenkins, G. M. and Watts, D. G., Spectral Analysis And Its Applications, Holden-Day, San Francisco, c. 1969.

well as upon (moving average) terms in the input -- n_t and n_{t-1}.

For the required autospectrum of x_t, n_t must be white. Thus,

$$E[n_t n_{t-k}] = 0, \; k \neq 0$$

$$= \sigma_n^2, \; k = 0. \tag{4.10}$$

Furthermore, future values of the input are uncorrelated with the present value of the output, i.e.,

$$E[n_{t+k} x_t] = 0, \; k>0. \tag{4.11}$$

Ratio of Output to Input Variances.

In selecting the value of noise (input) variance to yield a particular output variance, it is necessary to know the ratio of output to input variances of the filter. An expression for this ratio will be derived. We employ a notation used by Jenkins, Op. Cit., [11] for, respectively, the autocovariance and crosscovariance functions:

$$\gamma_{xx}(k) = E[x_t x_{t-k}]$$

$$\gamma_{xn}(k) = E[x_t n_{t-k}]. \tag{4.12}$$

In this notation, one desires

$$\gamma_{xx}(0)/\sigma_n^2 \text{ or } \gamma_{xx}(0)/\gamma_{nn}(0).$$

This result is obtained from (4.7) by successive multiplication of both sides by x_{t-1}, n_t, and n_{t-1}; and, then, by taking the mathematical expectation on both sides in all equations. This produces:

$$\gamma_{xx}(1) = -b_1\gamma_{xx}(0) - b_2\gamma_{xx}(1) + a_1\gamma_{xn}(0) + a_2\gamma_{xn}(1)$$

and

$$\gamma_{xn}(0) = a_o\sigma_n^2$$

$$\gamma_{xn}(1) = (a_1 - b_1 a_o)\sigma_n^2 \ .$$

Thus,

$$b_1\gamma_{xx}(0) + (1 + b_2)\ \gamma_{xx}(1) =$$

$$[a_o a_1 + a_2(a_1 - b_1 a_o)]\ \sigma_n^2 \ . \qquad (4.13)$$

After squaring both sides of (4.9) and taking expected values, one obtains

$$(1 - b_1^2 - b_2^2)\ \gamma_{xx}(0) - 2\ b_1 b_2\ \gamma_{xx}(1) =$$

$$\sigma_n^2[-2a_o a_1 b_1 - 2a_o a_2 b_2 - 2a_2 b_1(a_1 - b_1 a_o) + a_o^2 + a_1^2 + a_2^2]. \qquad (4.14)$$

One can solve (4.13) and (4.14) for the desired variance ratio.

$$\gamma_{xx}(0)/\gamma_{nn}(0) = \frac{C_1 B_2 - B_1 C_2}{A_1 B_2 - B_1 A_2} \ , \qquad (4.15a)$$

with

$$A_1 = b_1$$

$$A_2 = 1 - b_1^2 - b_2^2$$

$$B_1 = 1 + b_2$$

$$B_2 = -2\ b_1 b_2$$

$$C_1 = a_o a_1 + a_2(a_1 - b_1 a_o)$$

$$C_2 = -2a_o a_1 b_1 - 2a_o a_2 b_2 - 2a_2 b_1(a_1 - b_1 a_o) + a_o^2 + a_1^2 + a_2^2. \qquad (4.15b)$$

For numerical stability the denominator of the r.h.s. of (4.15a) must, of course, be non-zero. This implies that the parameters b_1 and b_2 must

lie within the region defined by:

$$|b_2| < 1$$

$$b_1 - b_2 < 1$$

and

$$b_1 + b_2 > -1.$$

This requirement is equivalent to the statement that the poles of (4.5) lie outside the unit circle. See Box, Op Cit, [10]. In practice, stability requirements are satisfied for the problem of modeling human tracker error using sampling rates of 10 or 20 hertz.

Summary.

To simulate the second-order, mean-zero component of a stochastic process having the desired cutoff frequency ν_t and standard deviation σ_t one can employ the digital filter given by (4.9) with a mean-zero, gaussian white-noise input n_t having a standard deviation given by

$$\sigma_n = [\gamma_{nn}(0)/\gamma_{xx}(0)]^{1/2} \sigma_t , \qquad (4.16)$$

with variance ratio given by (4.15) and with filter coefficients given by (4.6).

CHAPTER 5

AUTOSPECTRA OF THE DIGITAL ERROR PROCESSES

First Order Component

From the digital transfer function of the first-order process (equation (3.8a)),

$$H_z(z) = \frac{a_o(1+z^{-1})}{1 + bz^{-1}} \quad , \tag{5.1}$$

and with the following mapping into the frequency domain:

$$z = e^{j\omega T} = e^{j2\pi\nu T} \quad , \tag{5.2}$$

the squared modulus

$$H_1^2(\nu) = H_z(e^{j2\pi\nu T})\ H_z(e^{-j2\pi\nu T})$$

is

$$H_1^2(\nu) = \frac{2\ a_o^2\ (1 + \cos\ 2\pi\nu T)}{1 + b^2 + 2b\ \cos\ 2\pi\nu T} \quad , \tag{5.3}$$

with ν defined over positive frequencies from zero to the Nyquist frequency $\nu_f = 1/(2T)$.

The results in (5.1) and (5.3) were derived from a normalized analog transfer function having unity gain at frequency zero. Consequently, $H_1^2(0) = 1$. Then, the autospectrum of the first-order digital component, $\Gamma_{xx}(\nu)$, is given by

$$\Gamma_{xx}(\nu) = H_1^2(\nu)\ \Gamma_{nn}(\nu) \quad , \tag{5.4}$$

where $\Gamma_{nn}(\nu)$ is the autospectrum of the digital white noise (input) process, given by

$$\Gamma_{nn}(\nu) = \nu_f^{-1}\,\sigma_n^2\ ,\ 0 \le \nu \le \nu_f, \tag{5.5}$$

or, from (3.18),

$$\Gamma_{nn}(\nu) = 2T\,\sigma_s^2(a+1)/a \tag{5.6a}$$

or

$$\Gamma_{nn}(\nu) = \frac{2T(1+b)}{2\,a_o^2}\ \sigma_s^2\ ,\ 0 \le \nu \le \nu_f\ . \tag{5.6b}$$

The noise spectrum Γ_{nn} is comparable to the gain constant B in (1.10). As T approaches zero Γ_{nn} approaches B.

Example

It is interesting to compare the value of the first-order component autospectrum for the analog process (equation (1.6)) with that for the equivalent digital implementation. To this end, take the parameters of the example given previously in Chapter 1: ν_s=3 hz, σ_s=0.165 m. Assuming that the sampling rate (1/T) of the analog process is 20 hz,

T = 0.05 sec, and, by (3.6),

a = 0.509525.

From (3.8b),

a_o = 0.337540

b = -0.324920 .

Then, (5.3) becomes

$$H_1^2(\nu) = \frac{0.227866\ (1 + \cos\ 0.314159\nu)}{1.1055728 - 0.649839\ \cos\ 0.314159\nu}\ , \tag{5.7}$$

This result is compared with that of the corresponding analog process in Table 2. Additionally, squared modulii for other sampling rates are displayed in Table 2.

TABLE 2. COMPARISON OF THE ANALOG AND DIGITAL SQUARED MODULII OF THE FIRST-ORDER ERROR PROCESS

ν (hz)	$H_s^2(\nu)$ analog, B=1	$H_1^2(\nu)$, digital at sampling rate:		
		20 hz	40 hz	80 hz
0.0	1.0000	1.0000	1.0000	1.0000
0.3	0.9901	0.9915	0.9904	0.9902
0.5	0.9730	0.9767	0.9739	0.9732
1.0	0.9000	0.9119	0.9030	0.9007
1.5	0.8000	0.8183	0.8045	0.8011
2.0	0.6923	0.7109	0.6968	0.6934
3.0	0.5000	0.5000	0.5000	0.5000
4.0	0.3600	0.3297	0.3531	0.3583
6.0	0.2000	0.1205	0.1817	0.1955
8.0	0.1233	0.0267	0.0984	0.1171
10.0	0.0826	0.0000	0.0545	0.0755
$\Gamma_{nn}(\nu)$ (m^2/hz)	$5.777\ 10^{-3}$	$8.066\ 10^{-3}$	$7.031\ 10^{-3}$	$6.431\ 10^{-3}$

As noted from Table 2, the squared modulii of the analog and digital processes are in excellent agreement over the interval ($0 \leq \nu < \nu_f/2$). For frequencies within the interval ($\nu_f/2 \leq \nu \leq \nu_f$) and, particularly at the upper end of this interval, the autospectrum of the digital process departs significantly from that of the corresponding analog. Since there is no spectral content for the digital realizations above ν_f, i.e., all of the variance of the digital process must occur at frequencies below ν_f, the values of the digital autospectrum exceed those of the analog having the same variance for low frequencies. Thus, the autospectrum of a digital process produced by a low sampling rate (and low ν_f) will display substantial distortion relative to that of the corresponding analog process. This point is illustrated in Figure 3 in which different digital autospectra of the first-order stochastic process are compared to a corresponding analog autospectrum.

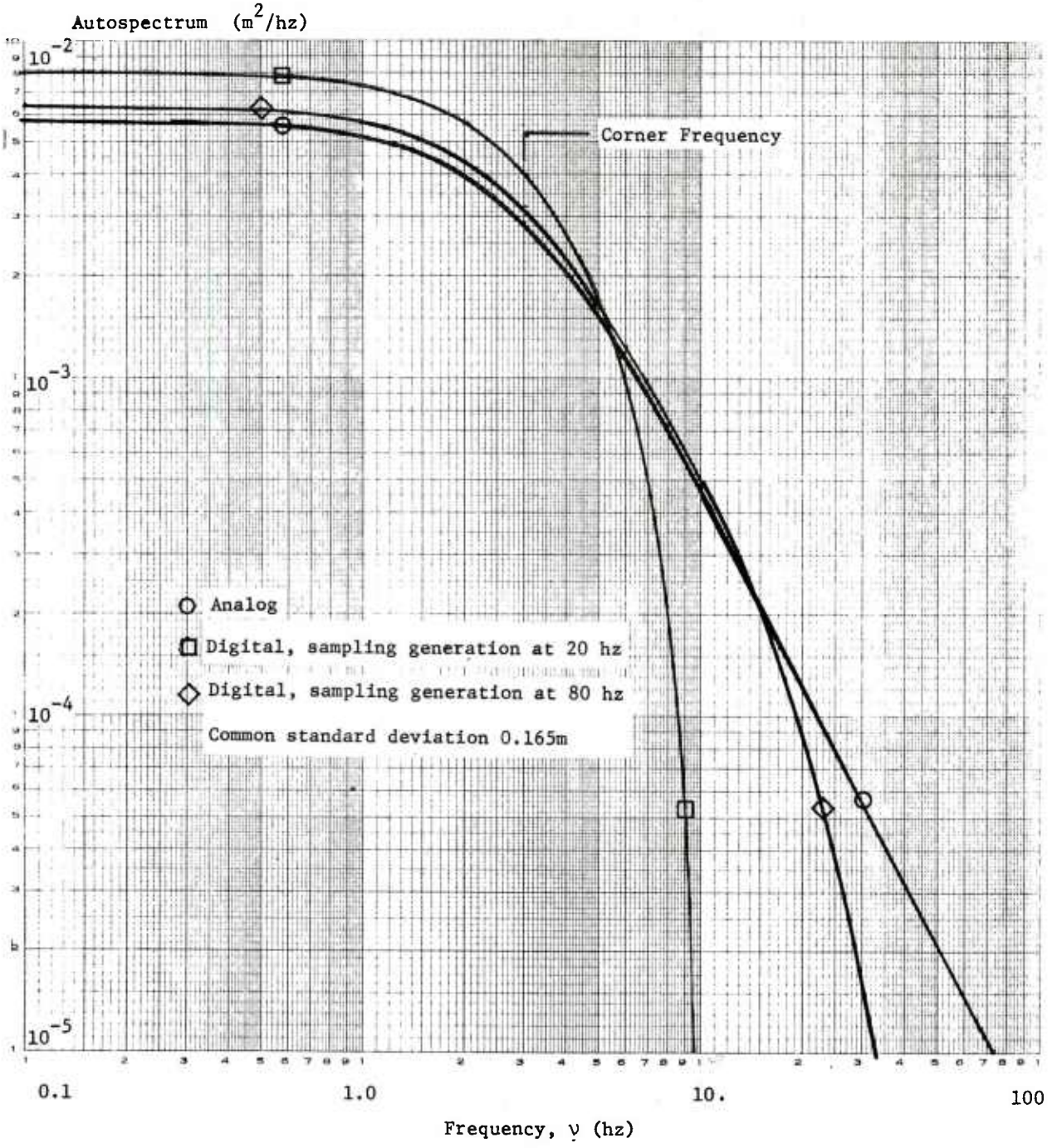

Figure 3. Comparison of the First-Order Autospectra for the Analog and Corresponding Digital Processes

Of course, if the contribution of the first-order process to the total spot motion variance is small, this distortion may be acceptable. However, if fidelity to the corresponding analog process is desired, a general rule might be that the sampling rate used in generating the process digitally should be 20 to 30 times the corner frequency. Naturally, the dynamical response of the system accepting this first-order noise is also a consideration in selecting a sampling generation rate.

Generally the dynamic components of a signal such as laser spot position are viewed only at discrete points in time, namely when the pulsed laser flashes. Thus, any spot motion due to a fundamentally continuous (analog) process is inherently time sampled. Further, this sampling interval T^* may be different from that used in the digital implementation, T. To quantitatively assess what effect the digital generation interval T has on the output series obtained by sampling at a time interval T^*, one must exploit some sampling theory. This theory is developed below for an ideal (delta-function) sampler and applied to the first-order component of the stochastic process.

The Transfer Function of a Time-Sampled Process

Whenever a stochastic process is sampled (or subsampled), the autospectrum of the sampled process may be substantially altered relative to the original process. This distortion will occur whenever the original process has an appreciable variance (or power) invested in frequencies (ν) above the Nyquist (or folding) frequency of the sampler. If the sampler is operating at a sampling rate $(T^*)^{-1}$, the folding frequency will be $\nu_f = (2T^*)^{-1}$ and variance in the original signal associated with $\nu > \nu_f$ will be confounded with the variance associated with ν for $0 \leq \nu < \nu_f$. In this section a theorem for ideal (point) samplers will be applied to several processes and examples will be offered to quantify the distortion accompanying sampling. In doing this, the author follows the notation and results of Kuo and Kaiser [12], p. 222 ff.

Notationally, let $f(nT^*)$ be the value of the original process evaluated at points in time: $t = nT^*$, with n an integer and T^* the constant sampling interval. Further, let $F(s)$ be the Laplace transform of the original process and let $F^*(s)$ be the Laplace transform of the sampled process, i.e., of the discrete series resulting from sampling. Then, for zero initial conditions,

$$F^*(s) = \Sigma_{n=-\infty}^{\infty} F(s + jn2\pi/T^*) \quad , \tag{5.8}$$

with $s = j\omega$ defined for $-\infty < \omega < \infty$.

---

[12] Kuo, F.F. and Kaiser, J.F. Systems Analysis by Digital Computer, John Wiley and Sons, New York, c. 1966.

And,

$$F^*(j\omega) = F(j\omega) + \Sigma_{n=1}^{\infty} F(j(\omega+\omega_n)) + \Sigma_{n=1}^{\infty} F(j(\omega-\omega_n)) \ , \tag{5.9a}$$

with

$$\omega_n = 2\pi n(T^*)^{-1} \tag{5.9b}$$

and

$$\omega = 2\pi\nu \ . \tag{5.9c}$$

Since the modulus of $F(j\omega)$ will generally decline with ω for values of ω greater than some value, say, ω^*, it will suffice to approximate F^* with a finite (and reasonably small) number of terms in the infinite sums. Thus,

$$F^*(j\omega) \cong F(j\omega) + \Sigma_{n=1}^{n^*} F(j(\omega+\omega_n)) + \Sigma_{n=1}^{n^*} F(j(\omega-\omega_n)). \tag{5.10}$$

In evaluating the autospectrum of the sampled process it will be convenient to separately find the real and imaginary parts of each of the terms in $F^*(j\omega)$.

Then,

$$\begin{aligned} \text{Re}\ \{F^*(j\omega)\} &\cong \text{Re}\ \{F(j\omega)\} \\ &+ \Sigma_{n=1}^{n^*} \text{Re}\ \{F(j(\omega+\omega_n))\} \\ &+ \Sigma_{n=1}^{n^*} \text{Re}\ \{F(j(\omega-\omega_n))\} \ , \end{aligned} \tag{5.11}$$

and likewise for the imaginary part of $F^*(j\omega)$, $\text{Im}\ \{F^*(j\omega)\}$.

Finally, the autospectrum of the sampled process is proportional to

$$|F^*(j\omega)|^2 = [\text{Re}\ \{F^*(j\omega)\}]^2 + [\text{Im}\ \{F^*(j\omega)\}]^2 \ . \tag{5.12}$$

As a particular application of the above results, take the first-order analog process, for which

$$F(s) = \omega_s\ (s + \omega_s)^{-1}. \tag{5.13}$$

In this case

$$F^*(j\omega) = \omega_s (j\omega + \omega_s)^{-1} + \omega_s \sum_{n=1}^{\infty} [j(\omega+\omega_n) + \omega_s]^{-1}$$

$$+ \omega_s \sum_{n=1}^{\infty} [j(\omega-\omega_n) + \omega_s]^{-1}. \qquad (5.14)$$

Separating F^* into real and imaginary parts:

$$\text{Re}\ \{F^*(j\omega)\} = [(\omega/\omega_s)^2 + 1]^{-1}$$

$$+ \sum_{n=1}^{\infty} [(\omega+\omega_n)^2/\omega_s^2 + 1]^{-1}$$

$$+ \sum_{n=1}^{\infty} [(\omega-\omega_n)^2/\omega_s^2 + 1]^{-1} \qquad (5.15)$$

and

$$-\text{Im}\ \{F^*(j\omega)\} = (\omega/\omega_s)\ [(\omega/\omega_s)^2 + 1]^{-1}$$

$$+ \sum_{n=1}^{\infty} ((\omega+\omega_n)/\omega_s)\ [(\omega+\omega_n)^2/\omega_s^2 + 1]^{-1}$$

$$+ \sum_{n=1}^{\infty} ((\omega-\omega_n)/\omega_s)\ [(\omega-\omega_s)^2/\omega_s^2 + 1]^{-1}\ . \qquad (5.16)$$

This case has been evaluated for the following specific parameters: ν_s = 1, 3 hz and T^* = 0.1, 0.05, 0.025 sec. The results are dispayed in Figures 4 and 5.

A second example of the effect of sampling is the case in which a digital implementation of a first-order process is subsampled, i.e., in which the sampling frequency $(T^*)^{-1}$ is a submultiple of the digital generation frequency T^{-1}. The digital process with transfer function $H_z(z)$ in equation (3.8a) will be the example taken here:

$$H_z(z) = \frac{a_o(1 + z^{-1})}{1 + bz^{-1}}\ . \qquad (5.17)$$

With the mapping into the s-plane:

$$z = e^{sT}\ , \qquad (5.18)$$

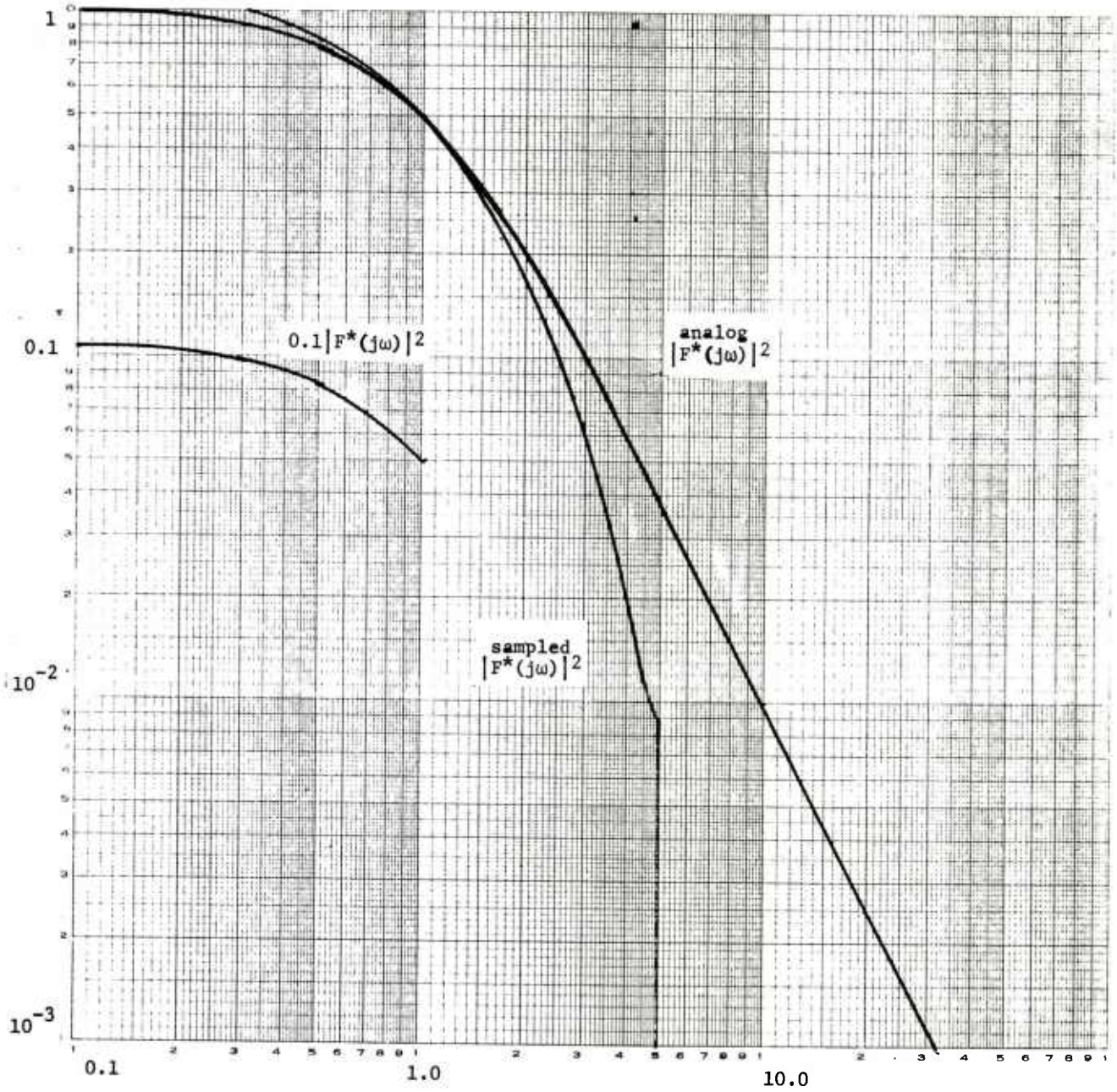

Figure 4. Comparison of a First-Order Analog Squared Modulus With the Squared Modulus of the Ideal Time-Sampled Series (Parameters: ν_s = 1 hz, T^* = 0.1 sec)

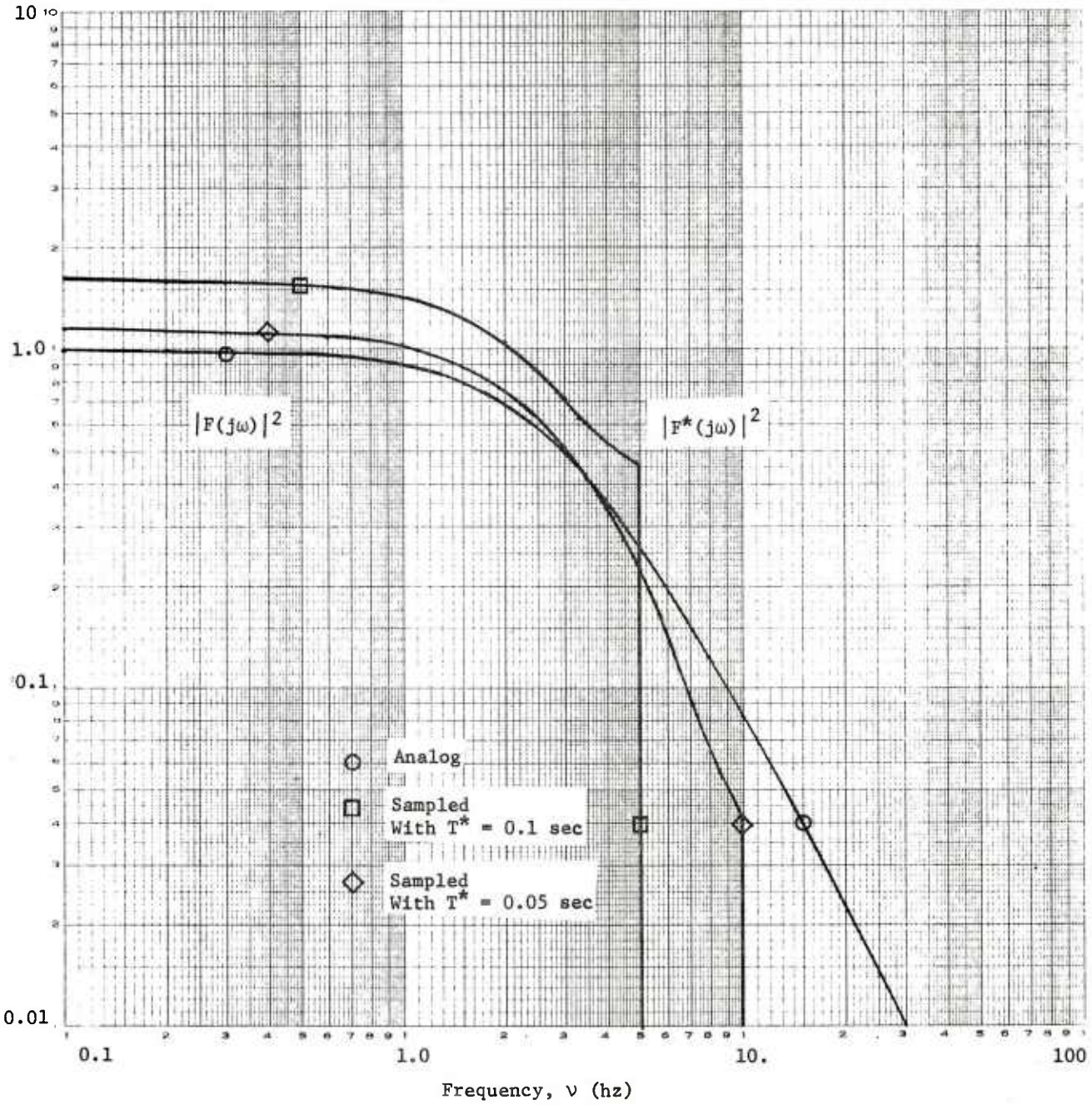

Figure 5. Comparison of a First-Order Analog Squared Modulus With the Squared Modulus of the Ideal Time-Sampled Series
(Parameters: ν_s = 3 hz, T^* = 0.05, 0.1 sec)

$$F(s) = H_z\,(e^{sT}) = \frac{a_o(1 + e^{-sT})}{1 + b\,e^{-sT}} \quad . \tag{5.19}$$

And,

$$F(j\omega) = \frac{a_o(1 + \exp(-j\omega T))}{1 + b\,\exp(-j\omega T)} \quad , \tag{5.20a}$$

with (from (3.8b))

$$a_o = a/(a + 1)$$

$$b = (a - 1)/(a + 1)$$

$$a = \tan\,(\pi\nu_s T) \quad . \tag{5.20b}$$

In this case,

$$\mathrm{Re}\,\{F(j\omega)\} = \frac{a_o\,(1 + b)(1 + \cos\,\omega T)}{1 + b^2 + 2\,b\,\cos\,\omega T} \tag{5.21a}$$

and

$$-\mathrm{Im}\,\{F(j\omega)\} = \frac{a_o\,(1 - b)\,\sin\,\omega T}{1 + b^2 + 2\,b\,\cos\,\omega T} \quad , \tag{5.21b}$$

for $-\pi \leq \omega T \leq \pi$; and when ωT is outside of this region, $F(j\omega)$ is identically zero.

Obviously, the sampling interval T^* must be an integral multiple of the generation interval T:

$$T^* = mT \quad , \quad m = 1, 2, 3 \ldots$$

In this example $F^*(j\omega)$ is evaluated for $\nu_s = 3$ hz and T = 0.025 and T = 0.05 sec with m = 2. Results are plotted in Figures 6 and 7. The autospectra for the time-sampled process in Figure 7 may be compared with the unsampled autospectra shown in Figure 3. The effect of sub-sampling order (m) on the squared modulus is shown in Table 3.

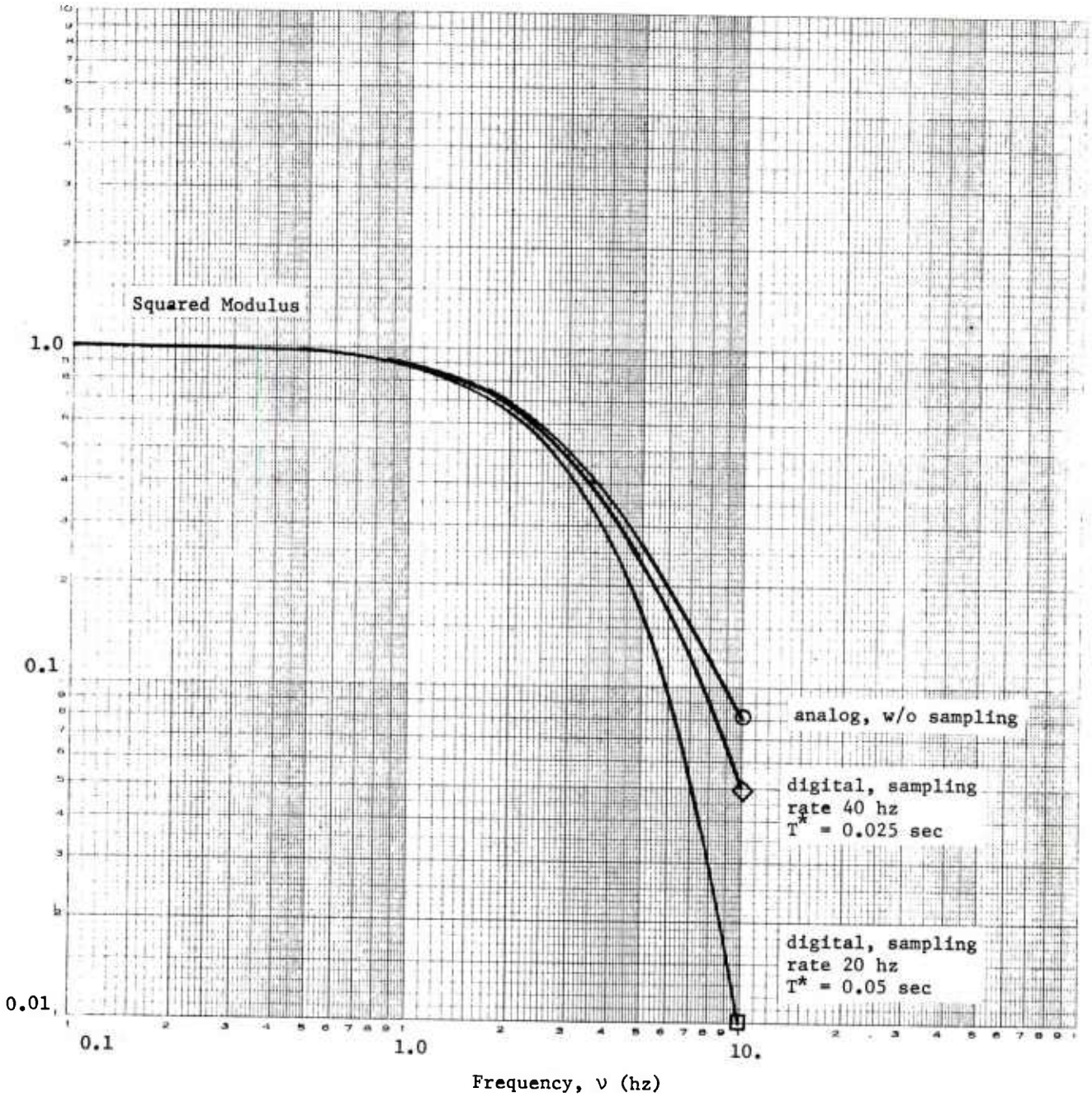

Figure 6. Comparison of Squared Modulii for Subsampled Digitally Generated First-Order Processes Having Different Sampling Rates (Parameters: ν_s = 3 hz, T = $T^*/2$)

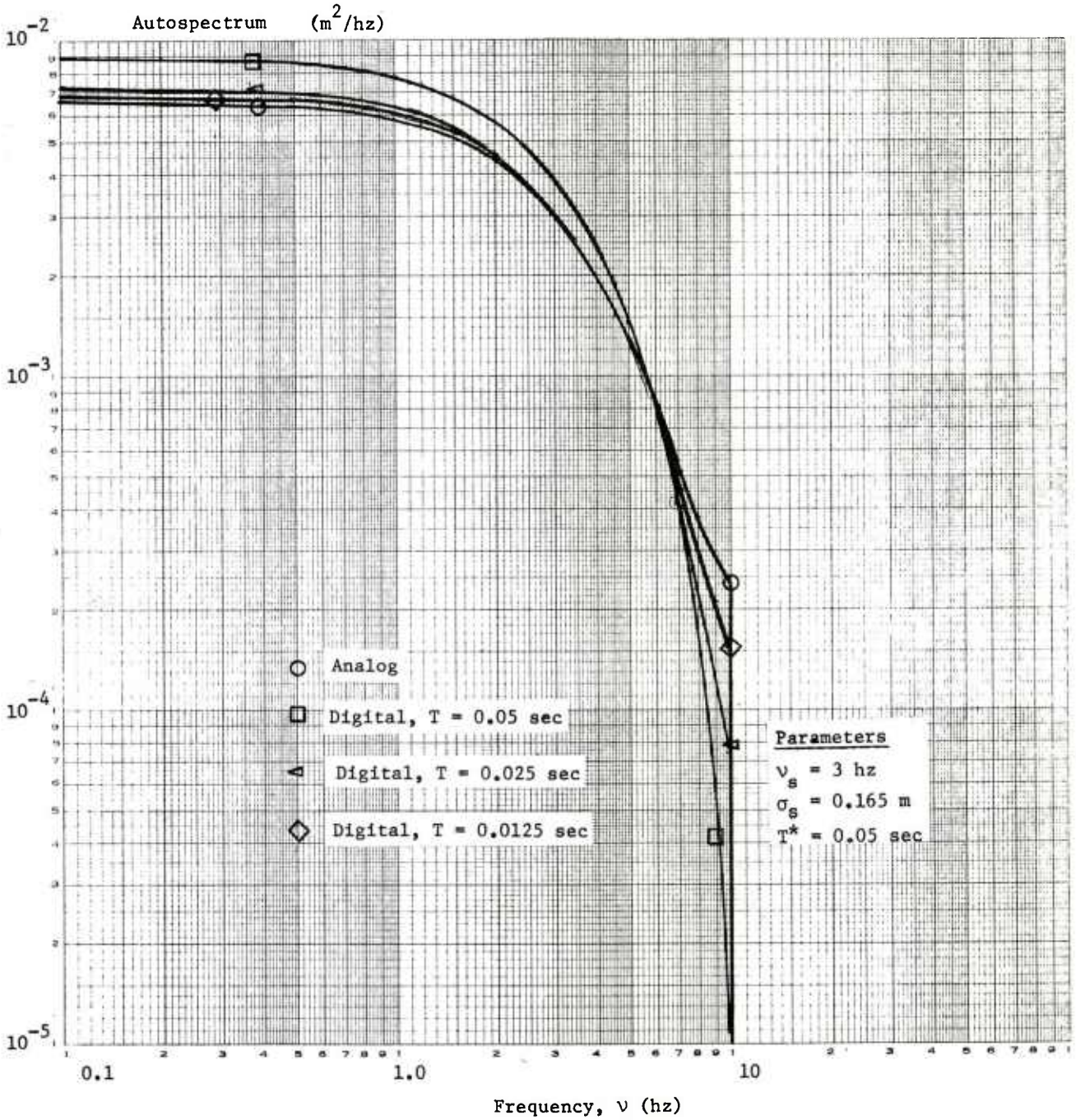

Figure 7. Comparison of the Autospectra of Time-Sampled Processes: Analog and Digital Implementations (Parameters: ν_s = 3 hz, σ_s = 0.165 m, T^* = 0.05 sec)

TABLE 3. EFFECT OF SUBSAMPLING ON THE SQUARED MODULUS OF A DIGITAL IMPLEMENTATION OF A FIRST-ORDER DYNAMIC PROCESS SAMPLED AT 20 HZ

Parameters: ν_s = 3 hz, T^* = 0.05 sec

ν (hz)	digital $\|F(j\omega)\|^2$ with $T = T^*/m$ subsampling order m			
	1	2	3	4
0.1	0.9987	0.9987	1.0311	1.0537
0.2	0.9949	0.9950	1.0272	1.0497
0.3	0.9887	0.9887	1.0208	1.0432
0.4	0.9800	0.9801	1.0120	1.0342
0.5	0.9690	0.9692	1.0008	1.0229
0.6	0.9560	0.9562	0.9875	1.0093
0.7	0.9409	0.9412	0.9721	0.9937
0.8	0.9240	0.9440	0.9549	0.9762
1.0	0.8855	0.8861	0.9157	0.9363
1.2	0.8420	0.8430	0.8714	0.8913
1.5	0.7709	0.7724	0.7991	0.8177
2.0	0.6475	0.6500	0.6737	0.6901
2.5	0.5306	0.5342	0.5551	0.5694
3.0	0.4276	0.4323	0.4507	0.4632
3.5	0.3406	0.3463	0.3625	0.3735
4.0	0.2687	0.2753	0.2898	0.2995
4.5	0.2100	0.2174	0.2305	0.2392
5.0	0.1624	0.1704	0.1824	0.1902

Aside from the distortions in the autospectrum (and process dynamics) due to digital sampling, there are distortions in the spectral estimates created by the statistical techniques employed in analyzing time series data. These distortions are discussed below.

The Effect of Lag Window in the Estimated Autospectrum

In estimating an autospectrum from time series data, it is essential to provide a means of averaging or smoothing spectral estimates to insure stochastic convergence as the length of the series (or record) grows indefinately large. For a single record, x(t), the smoothing is efficiently done by applying a weight function or "lag window", w(t), to the estimated autocovariance function, $\hat{\gamma}_{xx}(t)$, before taking the Fourier transform to form the smoothed autospectrum, $\hat{\Gamma}_{xx}(\omega)$. See Jenkins and Watts, 1968, Op Cit, [11]. Thus, for a continuous record of length t_e,

$$\hat{\Gamma}_{xx}(\omega) = \frac{2}{\pi} \int_0^{t_e} \hat{\gamma}_{xx}(t)\, w(t) \cos \omega t \, dt. \tag{5.22}$$

Without applying a weight function to the theoretical autocovariance, and for an essentially infinite record, one would obtain the theoretical (unsmoothed) autospectrum:

$$\Gamma_{xx}(\omega) = \frac{2}{\pi} \int_0^{\infty} \gamma_{xx}(t) \cos \omega t \, dt. \tag{5.23}$$

Parenthetically, it is noted that the spectrum is often expressed in terms of the natural frequency ν rather than the angular frequency ω. Then,

$$\Gamma'_{xx}(\nu) = \Gamma_{xx}(\omega(\nu)) \left|\frac{d\omega}{d\nu}\right|$$

$$\Gamma'_{xx}(\nu) = 2\pi \Gamma_{xx}(2\pi\nu) . \tag{5.24}$$

Altho smoothing is required to reduce the variance of the estimated autospectrum, it does create a distortion of the estimate $\hat{\Gamma}_{xx}(\omega)$ relative to $\Gamma_{xx}(\omega)$. It is the purpose of the developments of this section to quantify this distortion.

Two weight functions are frequently used in smoothing: one due to Bartlett--

$$w_B(t) = 1 - t/\tau_m \quad , \; 0 \leq t \leq \tau_m$$
$$= 0 \quad , \quad t > \tau_m \; , \tag{5.25}$$

where τ_m is a lag parameter, and one due to Tukey--

$$w_T(t) = \frac{1}{2}\,(1 + \cos(\pi t/\tau_m)), \; 0 \leq t \leq \tau_m$$
$$= 0 \quad t > \tau_m \; . \tag{5.26}$$

In the following analysis the simpler, Bartlett window is used. However, the effect shown on the estimated autospectrum is representative of several lag windows. Also in this analysis we take the estimated autocovariance function to be the theoretical autocovariance of a first-order analog process: $\gamma_{xx}(t) = \gamma_{xx}(0) \exp(-\lambda t)$. Specifically, from the second term of (2.11), the autocovariance of the scintillation process is

$$\gamma_{xx}(t) = \sigma_s^2 \, e^{-\omega_s t} \tag{5.27}$$

Then, for the Bartlett weight function, the smoothed autospectrum is

$$\hat{\Gamma}_{xx}(\omega) = \frac{2\sigma_s^2}{\pi} \int_0^{\tau_m} \cos(\omega t) \, e^{-\omega_s t} \, (1 - t/\tau_m) \, dt. \tag{5.28}$$

$$\hat{\Gamma}_{xx}(\omega) = \frac{2\sigma_s^2}{\pi\,\omega_s} \int_0^{\omega_s \tau_m} \cos\left(\frac{\omega}{\omega_s} x\right) e^{-x} \left(1 - \frac{x}{\omega_s \tau_m}\right) dx \; . \tag{5.29}$$

From (1.10), the constant multiplier on the r.h.s. of (5.29) is $B/2\pi$.

$$\frac{2\pi}{B}\,\hat{\Gamma}_{xx}(\omega) = \int_0^{\omega_s\tau_m} \cos\left(\frac{\omega}{\omega_s}\,x\right)\, e^{-x}\, dx$$

$$- \frac{1}{\omega_s\tau_m} \int_0^{\omega_s\tau_m} x e^{-x} \cos\left(\frac{\omega}{\omega_s}\,x\right)\, dx. \qquad (5.30)$$

After some manipulation,

$$\frac{2\pi}{B}\,\hat{\Gamma}_{xx}(\omega) = \bar{\Gamma}_{xx}(\omega) + \alpha(\omega)$$

$$+ e^{-\omega_s\tau_m}\,[\alpha(\omega)\,\cos\,\omega\tau_m + \beta(\omega)\,\sin\,\omega\tau_m]\,, \qquad (5.31a)$$

where

$$\bar{\Gamma}_{xx}(\omega) = (1 + (\omega/\omega_s)^2)^{-1}$$

$$\alpha(\omega) = \omega_s\tau_m^{-1}\,(\omega_s^2 - \omega^2)\,(\omega_s^2 + \omega^2)^{-2}$$

$$\alpha(\omega) = \frac{1 - (\omega/\omega_s)^2}{\omega_s\tau_m\,(1 + (\omega/\omega_s)^2)^2}\,.$$

$$\beta(\omega) = -\,2\,\omega_s^2\tau_m^{-1}\omega(\omega_s^2 + \omega^2)^{-2}$$

$$\beta(\omega) = -2\,(\omega/\omega_s)(\omega_s\tau_m)^{-1}\,(\bar{\Gamma}_{xx}(\omega))^2\,. \qquad (5.31b)$$

Note that the normalized smoothed autospectrum $(2\pi/B)\,\hat{\Gamma}_{xx}$ approaches the unsmoothed function $\bar{\Gamma}_{xx}$ as τ_m grows infinite. Some numerical examples of $\hat{\Gamma}$ were evaluated for several values of the parameters ν_s (or ω_s) and τ_m. Results are displayed in Figures 8 and 9. The effect of smoothing is to shift variance (or power) to lower frequencies and to introduce a damped oscillatory term. These distortions are not very significant for values of $\nu_s\tau_m$ greater than about 1.5.

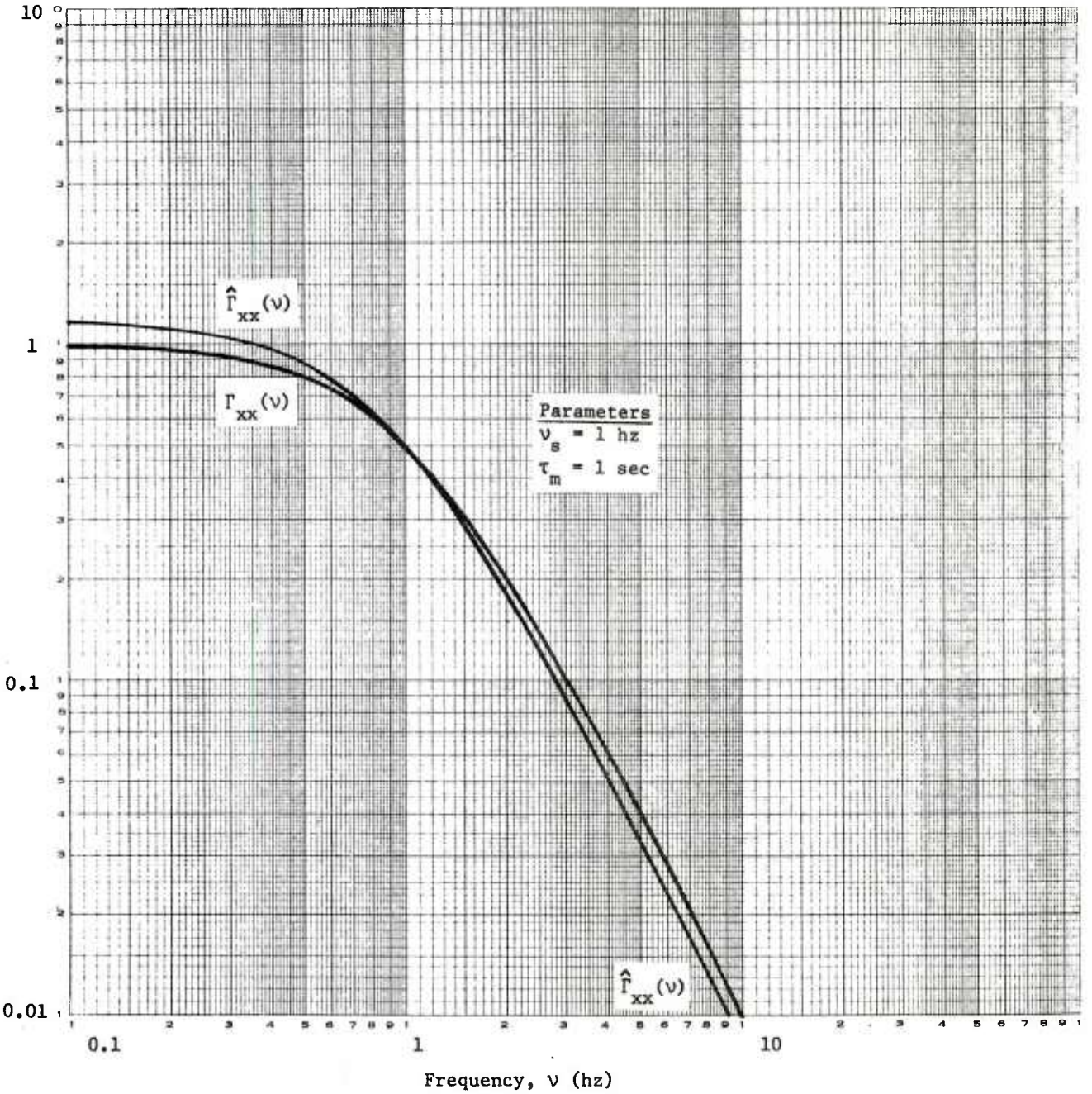

Figure 8. The Smoothed Autospectrum, $\hat{\Gamma}_{xx}(\nu)$, Due to a Bartlett Lag Window Applied to a First-Order Autocovariance With Associated Theoretical (Unsmoothed) Spectrum $\Gamma_{xx}(\nu)$, (Parameters: ν_s = 1 hz, τ_m = 1 sec)

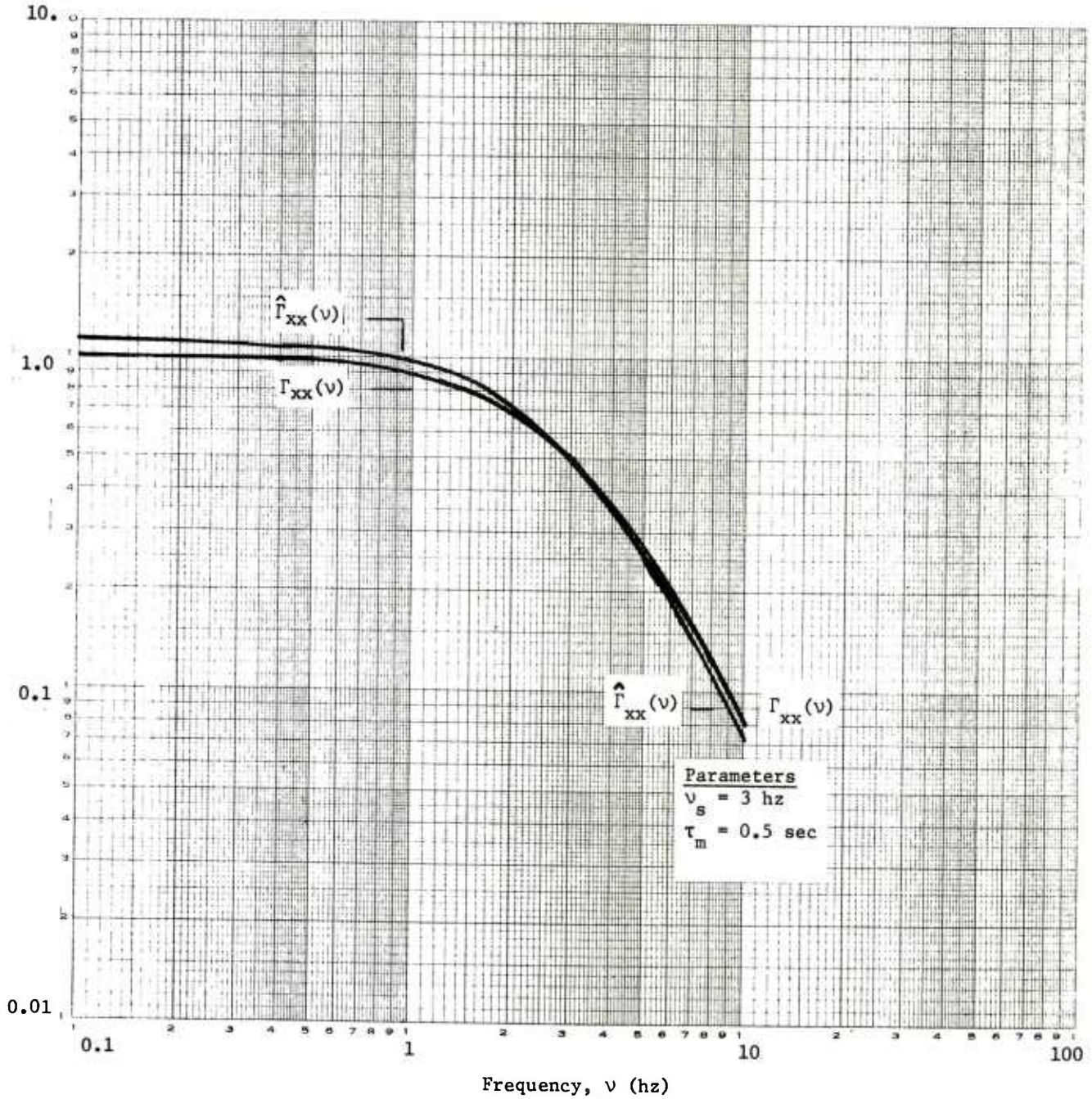

Figure 9. The Smoothed Autospectrum, $\hat{\Gamma}_{xx}(\nu)$, Due to a Bartlett Lag Window Applied to a First-Order Autocovariance With Associated Theoretical (Unsmoothed) Spectrum $\Gamma_{xx}(\nu)$ (Parameters: ν_s = 3 hz, τ_m = 0.5 sec)

Second-Order Component

The digital transfer function used in describing the second-order, tracking component of the laser spot motion (equation (4.5)) is repeated here.

$$H_z(z) = \frac{a_o + a_1 z^{-1} + a_2 z^{-2}}{1 + b_1 z^{-1} + b_2 z^{-2}} \quad . \tag{5.32}$$

The autospectrum of the process is proportional to the squared modulus $|H_z(\exp(j\omega T))|^2$. Notationally,

$$H_2^2(\omega) = |H_z(e^{j\omega T})|^2 = |H_z(e^{j2\pi\nu T})|^2, \tag{5.33}$$

with sampling generation interval T.

Using De Moivre's theorem,

$$e^{j\omega T} = \cos \omega T + j \sin \omega T, \tag{5.34}$$

with (5.32) and (5.33),

$$H_2^2(\omega) = [(a_o + a_1 \cos \omega T + a_2 \cos 2\omega T)^2 + (a_1 \sin \omega T + a_2 \sin 2\omega T)^2]/$$

$$[(1 + b_1 \cos \omega T + b_2 \cos 2\omega T)^2 + (b_1 \sin \omega T + b_2 \sin 2\omega T)^2]. \tag{5.35}$$

Using equation (4.6) and after some manipulation, (5.35) becomes

$$H_2^2(\omega) = \frac{\omega_a^4 (3 + 4 \cos \omega T + \cos 2\omega T)}{3(\omega_a^4 + 1) + 4(\omega_a^4 - 1) \cos \omega T + (\omega_a^4 + 1) \cos 2\omega T} \quad , \tag{5.36}$$

where

$$\omega_a = \tan (\pi \nu_t T). \tag{5.37}$$

Either (5.35) or (5.36) can be used to evaluate the squared modulus of the second-order dynamic component. Altho (5.36) has a simpler form than (5.35), computational experience using single-precision arithmetic on the IBM 360 series computers has demonstrated that (5.36) is somewhat more sensitive to truncation error than (5.35). In fact, it is noted

that generally all second-order transfer functions and squared modulii are more sensitive to loss of precision due to arithmetic truncation than are their first-order counterparts. When using IBM 360 computers it is recommended that double-precision arithmetic be used.

The above expressions for the second-order squared modulus are normalized so that $H_2^2(0) = 1$. To calculate the autospectrum, $\Gamma_{xx}(\nu)$, of the second-order (tracking) process, one employs:

$$\Gamma_{xx}(\nu) = H_2^2(2\pi\nu)\ \Gamma_{nn}(\nu)\ , \tag{5.38}$$

where $\Gamma_{nn}(\nu)$ is the input noise spectrum to the second-order digital filter. The noise spectrum is a function of the sampling generation interval, T, and the variance of the tracking process, σ_t^2:

$$\Gamma_{nn} = 2T\ \sigma_t^2\ [\gamma_{nn}(0)/\gamma_{xx}(0)]\ , \tag{5.39}$$

with the ratio of variances $\gamma_{nn}(0)/\gamma_{xx}(0)$ given by (4.15a).

As with the first-order process, it is useful to make numerical comparisons between the squared modulus of the digital implementation of the second-order (tracking) component and that of the corresponding analog process. The transfer function for a general second-order analog process, $H_t(s)$, is given by equation (4.1). The general squared modulus is, then,

$$H_t^2(j\omega) = 1/[(1 - (\omega/\omega_a)^2)^2 + 4\zeta^2\ (\omega/\omega_a)^2] \tag{5.40}$$

With the Butterworth assumption of $\zeta = 1/\sqrt{2}$ and with $\omega_a = 2\pi\nu_t$,

$$H_t^2(\nu) = 1/[1 + (\nu/\nu_t)^4]\ , \tag{5.41}$$

as in equation (1.1) with A = 1.

The analog gain constant A (equation (1.5)) represents the analog input noise spectrum and is comparable with Γ_{nn} given by (5.39). In fact,

$$\lim_{T\to 0} \Gamma_{nn} = A\ . \tag{5.42}$$

Example

Pursuing the example of Chapter 1, with

$$\nu_t = 0.7 \text{ hz}$$

$$\sigma_t = 0.23 \text{ m}$$

$$T = 0.1 \text{ sec},$$

$\omega_a = 0.219912$, and from (5.36):

$$H_2^2(\nu) = 2.33879\ 10^{-3}[3 + 4\cos(0.62832\nu) + \cos(1.25664\nu)]/[3.00716 - 3.99064\cos(0.62832\nu) + 1.002339\cos(1.25664\nu)]. \quad (5.43)$$

Numerical results from this expression and similar digital squared modulii calculated with T = 0.05 sec and 0.025 sec are compared with the analog squared modulus in Table 4. Spectral amplitudes for the noise are also shown in Table 4. Spectra are plotted in Figure 10.

TABLE 4. COMPARISON OF THE ANALOG AND DIGITAL SQUARED MODULII OF THE SECOND-ORDER (TRACKING) ERROR PROCESS

ν (hz)	analog $H_z^2(\nu)$ A=1	digital, $H_2^2(\nu)$ with T (sec):		
		0.025	0.05	0.10
0.1	1.000	1.000	1.000	1.000
0.2	0.993	0.993	0.993	0.994
0.3	0.967	0.967	0.968	0.969
0.4	0.904	0.904	0.905	0.907
0.5	0.793	0.794	0.794	0.799
0.6	0.649	0.650	0.650	0.653
0.7	0.500	0.500	0.500	0.500
0.8	0.370	0.369	0.368	0.365
1.0	0.194	0.193	0.191	0.183
1.2	0.104	0.103	0.101	0.092
1.5	0.0453	0.0447	0.0428	0.0357
2.0	0.0148	0.0144	0.0132	0.0089
3.0	0.00296	0.00275	0.00220	0.00070
5.0	0.00038	0.00031	0.00015	0.00000
$\Gamma_{nn}(\nu)$ (m^2/hz)	0.0680	0.0682	0.0685	0.0695

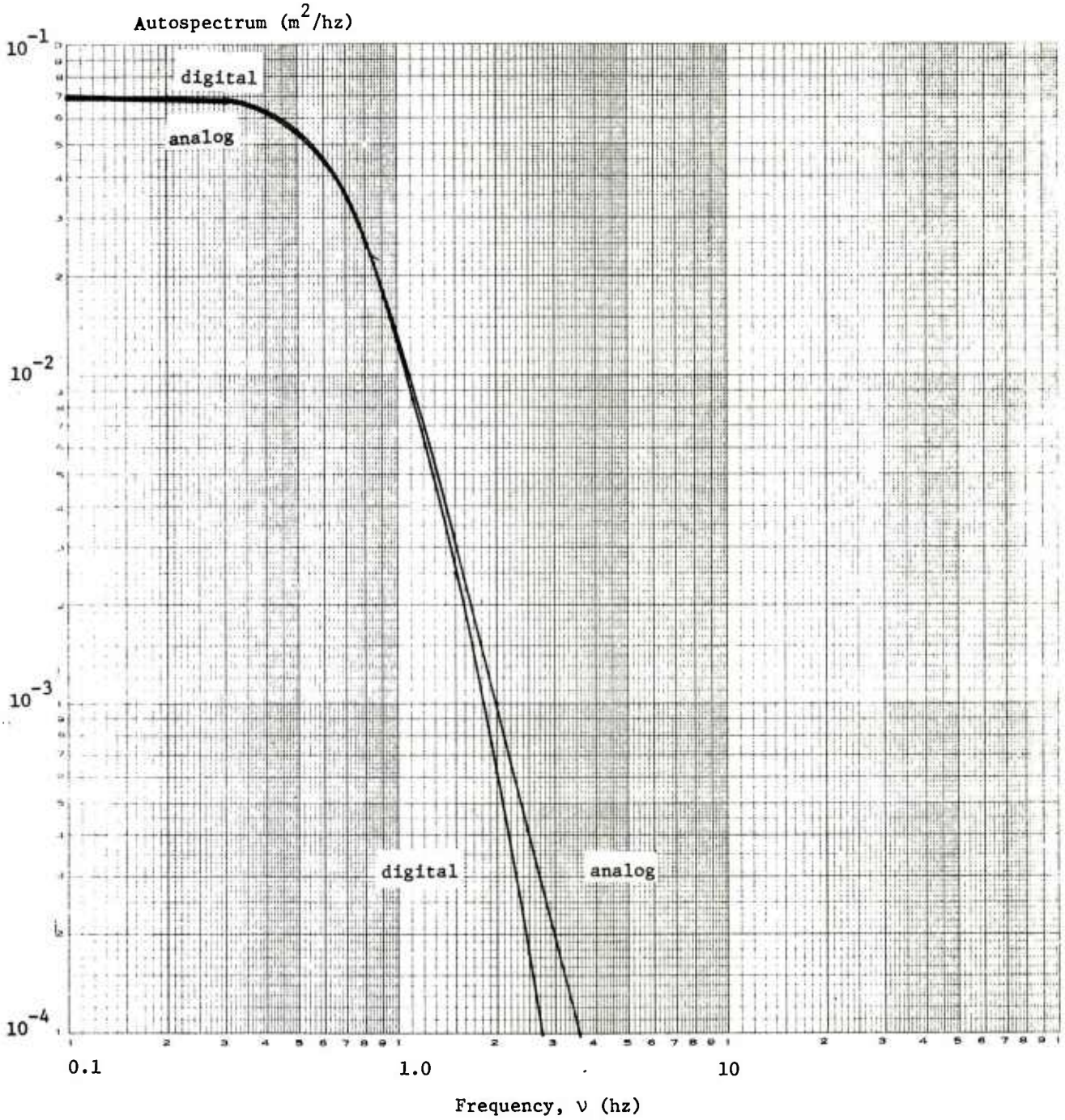

Figure 10. Autospectra of the Second-Order (Tracking) Process(Parameters: ν_t = 0.7 hz, σ_t = 0.230 m, T = 0.1 sec)

CHAPTER 6

SPECTRAL MOMENTS AND PARAMETER ESTIMATION

The spot motion process has been shown to consist of a mixture of first-and second-order dynamic components characterized by four parameters--the two crossover frequencies ν_s and ν_t and the two variances σ_s^2 and σ_t^2 or, alternatively, the spectral gain constants B and A. The existence of four parameters to estimate from the autospectrum suggests that expressions for the first four spectral moments (zeroth thru third) in terms of the four unknowns could be developed and used with experimental values of the spectral moments to solve for the estimates. This concept was explored and found to be impractically complex for a mixture of dynamic components. However, for evaluating processes having only one dynamic component, the concept of matching spectral moments to produce parameter estimates appears to have promise. The estimating relations for a pure Butterworth second-order process and for a pure first-order process are derived below.

Spectral Moments for the Second-Order Butterworth Process

The autospectrum for the continuous-time (analog) second-order Butterworth stochastic process $\{x(t)\}$ is given by

$$\Gamma_{xx}(\nu) = \frac{A}{1 + (\nu/\nu_t)^4}, \quad 0 \leq \nu < \infty, \tag{6.1a}$$

with

$$A = \frac{4\,\sigma_t^2}{\sqrt{2}\,\pi\,\nu_t}, \tag{6.1b}$$

By definition the k th spectral moment is given as

$$\lambda_k = \int_0^\infty \nu^k\, \Gamma_{xx}(\nu)\, d\nu,$$

or

$$\lambda_k = A\,\nu_t^{k+1} \int_0^\infty \frac{x^k\, dx}{1 + x^4}. \tag{6.2}$$

Using the general result:

$$\int_0^\infty \frac{x^{p-1}\,dx}{1+x^q} = (\pi/q)\,[1/\sin(p\pi/q)], \qquad (6.3)$$

$$1 \le p < q \ ,$$

$$\lambda_0 = A\,\nu_t\,(\tfrac{\pi}{4})\,\sqrt{2}$$

$$\lambda_1 = A\,\nu_t^2\,(\tfrac{\pi}{4})$$

$$\lambda_2 = A\,\nu_t^3\,(\tfrac{\pi}{4})\,(\sqrt{2}) \ . \qquad (6.4)$$

For all $k \ge 3$, the moments of the analog process are infinite. However, the parameters A and ν_t can be estimated using λ_0 and λ_1 as follows:

$$A = \frac{2}{\pi}\frac{\lambda_0^2}{\lambda_1} \qquad (6.5)$$

$$\nu_t = \frac{\sqrt{2}\,\lambda_1}{\lambda_0} \ . \qquad (6.6)$$

In practice A and ν_t would be developed by substituting the sample estimates $\hat{\lambda}_0$ (or $\hat{\sigma}_t^2$) and $\hat{\lambda}_1$ for λ_0 and λ_1, respectively.

The moments for a digital implementation of this process are, of course, finite. Let ν_f be the Nyquist (folding) frequency. Then, the digital moments are approximated by

$$\tilde{\lambda}_k = \int_0^{\nu_f} \nu^k\,\Gamma_{xx}(\nu)\,d\nu \qquad (6.7)$$

or

$$\tilde{\lambda}_k = A\,\nu_t^{k+1} \int_0^{\xi} \frac{x^k\,dx}{1+x^4} \ , \qquad (6.8)$$

where

$$\xi = \nu_f/\nu_t \ . \tag{6.9}$$

For notational convenience, define the k th normalized moment $\bar{\lambda}_k$ as

$$\bar{\lambda}_k = \tilde{\lambda}_k/(A\ \nu_t^{k+1}) \quad , \quad k \geq 0. \tag{6.10}$$

Then,

$$\bar{\lambda}_0 = \frac{1}{4\sqrt{2}} \left[\ell n\left(\frac{\xi^2 + \sqrt{2}\ \xi + 1}{\xi^2 - \sqrt{2}\ \xi + 1}\right) + 2\ \tan^{-1}\left(\frac{\sqrt{2}\ \xi}{1 - \xi^2}\right)\right]$$

$$\bar{\lambda}_1 = \frac{1}{2}\ \tan^{-1}(\xi^2)$$

$$\bar{\lambda}_2 = \frac{1}{4\sqrt{2}} \left[\ell n\left(\frac{\xi^2 - \sqrt{2}\ \xi + 1}{\xi^2 + \sqrt{2}\ \xi + 1}\right) + 2\ \tan^{-1}\left(\frac{\sqrt{2}\ \xi}{1 - \xi^2}\right)\right]$$

$$\bar{\lambda}_3 = \frac{1}{4}\ \ell n(1 + \xi^4) \quad . \tag{6.11}$$

Spectral Moments for the First-Order Process

The autospectrum for a first-order process {x(t)} with crossover frequency ν_s and gain constant B is given by

$$\Gamma_{xx}(\nu) = \frac{B}{1 + (\nu/\nu_s)^2} \ , \ 0 \leq \nu < \infty \ . \tag{6.12}$$

From the definition of spectral moment (equation (6.2)) and the general result of (6.3), it is seen that only the zeroth moment of the first-order process is finite:

$$\lambda_0 = \int_0^\infty \frac{B\ d\nu}{1 + (\nu/\nu_s)^2}$$

$$\lambda_0 = B(\pi/2) \quad . \tag{6.13}$$

As with the second-order process, define the moments of the digital implementation of the first-order process ($\tilde{\lambda}_k$) as definite integrals with the Nyquist frequency as the upper limit. Thus,

$$\tilde{\lambda}_k = \int_0^{\nu_f} \nu^k \, \Gamma_{xx}(\nu) \, d\nu$$

$$\tilde{\lambda}_k = B \, (\nu_s)^{k+1} \int_0^{\eta} \frac{x^k \, dx}{1 + x^2} \, , \tag{6.14}$$

with

$$\eta = \nu_f / \nu_s \quad . \tag{6.15}$$

The normalized moments for the first-order process are defined as

$$\bar{\lambda}_k = \tilde{\lambda}_k / (B \, \nu_s^{k+1}) \quad , \; k \geq 0. \tag{6.16}$$

For the first-order process,

$$\bar{\lambda}_0 = \tan^{-1}(\eta)$$

$$\bar{\lambda}_1 = \frac{1}{2} \ell n(1 + \eta^2)$$

$$\bar{\lambda}_2 = \eta - \tan^{-1}(\eta)$$

$$\bar{\lambda}_3 = \frac{\eta^2}{2} - \frac{1}{2} \ell n(1 + \eta^2) \quad . \tag{6.17}$$

By inspection of (6.16) and (6.17) one can write the following two equations which can be solved simultaneously for B and ν_s:

$$B = \frac{\ell n(1 + \eta^2)}{2[\tan^{-1}(\eta)]^2} \left(\tilde{\lambda}_0^2/\tilde{\lambda}_1\right) \tag{6.18}$$

$$\eta = \nu_f[(B\ \nu_f - \tilde{\lambda}_0)/\tilde{\lambda}_2]^{1/2}, \tag{6.19}$$

with

$$\nu_s = \nu_f/\eta \quad .$$

REFERENCES

1. Memorandum for Record, AMSAR-SAM, 23 July 1975, subject: Army-Navy Guided Projectile Effectiveness Study.

2. Schlenker, G. J. and Heider, R. D., Distribution of Angle of Obliquity of Laser-Guided Projectiles With Respect to the Target at Impact, Report No. DRSAR/SA/N-51, (AD A032683), U.S. Army Armament Command, Rock Island, IL, August 1976.

3. Pastrick, H. L. and Hollman, H. C., Analysis and Digital Simulation Models for CLGP: Martin Marietta Aerospace Design, Report No. RG-75-29, (Appendix G, Pulse Dropout and Pulse Dither Subroutines), U.S. Army Missile Command, Huntsville, AL, Dec 1974.

4. Letter, AMSAR-SA, 10 Dec 74, subject: Reduction and Analysis of CLGP-OT-1 Tracking Data.

5. Schlenker, G. J., "Proportion of Energy Spilled Over a Target During Tracking With a Laser Designator and Implications for Terminal Guidance," Systems Analysis Directorate Activities Summary November 1976, Report No. DRSAR/SA/N-60, U.S. Army Armament Command, Rock Island, IL, December 1976.

6. Minutes of a Meeting at White Sands Missile Range, NM, STEWS-TE-AG, 18 June 1976, subject: Uniform Standards for Laser Designator Developments.

7. Wolfe, W. L. (Ed) Handbook of Military Infrared Technology, Office of Naval Research, Washington, D.C. c. 1965.

8. Walsh, P. J., A Study of Digital Filters, AD710381, Naval Postgraduate School, Monterey, CA., Dec 1969.

9. Stanley, W. D. Digital Signal Processing, Reston Pub. Co., Inc., Reston, VA., c. 1975.

10. Box, G. E. P. and Jenkins, G. M., Time Series Analysis: Forecasting and Control, Holden-Day, San Francisco, c. 1970.

11. Jenkins, G. M. and Watts, D. G., Spectral Analysis and Its Applications, Holden-Day, San Francisco, c. 1969.

12. Kuo, F. F. and Kaiser, J. F. Systems Analysis by Digital Computer, John Wiley and Sons, New York, c. 1966.

APPENDIX A
SUBROUTINE TO GENERATE LASER SPOT MOTION

Subroutines SPOTIN and SPOTMO--an entry point in SPOTIN--generate spot motion in azimuth and elevation coordinates for use in laser signature models. SPOTIN initializes the program SPOTMO by providing azimuth and elevation standard deviations for both the tracking and scintillation stochastic components as well as the crossover (corner) frequencies of each of the components. The sampling generation interval is also specified. For subsampling, subroutine SPOTMO is called several times for each repetition of the laser interpulse interval. Thus, the sampling generation interval must be chosen in a manner appropriate to the use of this routine. SPOTIN computes the filter coefficients for the tracking component by means of equation (4.6) and the coefficients for the scintillation (first-order) component via (3.8b).

The input requirements of both SPOTIN and SPOTMO are specified in the following source program listing. Output from SPOTMO is also specified in that listing. In operation SPOTIN is called only once for initialization and SPOTMO is called where the output position array is required, typically nested in a loop of the calling program.

```
C<<<<<<<<<<<<<<<<<<<<<<<<<<<<<  SPOTIN  >>>>>>>>>>>>>>>>>>>>>>>>>>>>>>>>
C--  SPOT MOTION DRIVER WITH SCINTILLATION >>>>>>>>>>>>>>>>>>>>>>>>>>>>>>
      SUBROUTINE SPOTIN (SIGMA, CF, DT)
      INTEGER TR/1/, SC/2/, AZ/1/, EL/2/
      DIMENSION SIGMA(2,2), CF(2)
C--  SPOTIN INITIALIZES THE ROUTINE SPOTMO FOR THE 2-DIMENSIONAL (AZI-
C    MUTH & ELEVATION) MOTION OF THE DESIGNATOR BEAM ABOUT THE DESIRED
C    DIRECTION.
C    INPUT REQUIREMENTS:
C    *     SIGMA -- ARRAY OF STANDARD DEVIATIONS OF ERROR COMPONENTS.
C                   UNITS SAME AS "OUTPUT" OF SPOTMO, BELOW.
C          SIGMA(1,1) = SIGMA(AZ,TR) = S. D. IN AZIM OF TRACKING PROCESS.
C          SIGMA(2,1) = SIGMA(EL,TR) = S. D. IN ELEV OF TRACKING PROCESS.
C          SIGMA(1,2) = SIGMA(AZ,SC) = S. D. IN AZIM OF SCINT PROCESS.
C          SIGMA(2,2) = SIGMA(EL,SC) = S. D. IN ELEV OF SCINT PROCESS.
C    *     CF -- VECTOR OF CORNER FREQUENCIES OF PROCESSES (HZ).
C          CF(1) = CF(TR) = C. F. FOR TRACKING
C          CF(2) = CF(SC) = C. F. FOR SCINTILLATION
C    *     DT -- SAMPLING INTERVAL (SEC)
C
      DIMENSION XT(2,3), ZT(2,3), XS(2,2), ZS(2,2), OUTPUT(2,3)
      DATA PI / 3.141593 /, NET /3/
C
C--  CHECK FOR PRESENCE OF TRACKING ERROR
C
      ITRACK = 0
      IF ( ((SIGMA(AZ,TR).LE.0.).AND.(SIGMA(EL,TR).LE.0.)) .OR.
     1     (CF(TR).LE.0.) )   GO TO 150
      ITRACK = 1
C--  TRACKING ERROR IS PRESENT
C--  CLEAR TRACKING NOISE ARRAYS AND COMPUTE FILTER COEFFICIENTS
      DO 100 I= AZ, EL
      DO 100 J=I,3
      XT(I,J) = 0.
  100 ZT(I,J) = 0.
      ZETAAL = SQRT(0.5)
      OMEGAA = TAN(PI*CF(TR)*DT)
      DUMMY = 1. /(1. + OMEGAA*(2. *ZETAAL + OMEGAA) )
      A0 = OMEGAA**2 * DUMMY
      A1 = A0 + A0
      B1 = 2. * (OMEGAA**2 - 1. ) * DUMMY
      B2 = (1. - OMEGAA*(2. *ZETAAL - OMEGAA) ) * DUMMY
      SDNT = SQRT( (B2-1.)*((B2+1.)**2 - B1*B1) / (A0*A1*((B2-1.)**2 -
     1     (B1-2.)**2)) )
      TMAX = 5.*SDNT
      TMIN = -TMAX
  150 CONTINUE
C
C--  CHECK FOR PRESENCE OF SCINTILLATION
C
      ISCINT = 0
      IF ( ((SIGMA(AZ,SC).LE.0.).AND.(SIGMA(EL,SC).LE.0.)) .OR.
     I     (CF(SC).LE.0.) )   GO TO 250
      ISCINT = 1
C--  SCINTILLATION IS PRESENT
C--  CLEAR SCINTILLATION NOISE ARRAYS AND COMPUTE FILTER COEFFICIENTS
      DO 200 I = AZ, EL
      DO 200 J = I,2
      XS(I,J) = 0.
  200 ZS(I,J) = 0.
```

```
      OMEGAA = TAN(P1*CF(SC)*DT)
      AA0 = OMEGAA / (OMEGAA+1.)
      BB = (OMEGAA-1.) / (OMEGAA+1.)
      SDNS = SQRT(1. + 1./OMEGAA)
      SMAX = 5.*SDNS
      SMIN = -SMAX
  250 CONTINUE
      RETURN
C
      ENTRY SPOTMO (NFWD, ISEEDT, ISEEDS, OUTPUT)
 1001 FORMAT('0***ERROR -- ', I10, '-TIME-STEP ADVANCE CALLED FOR IN SPO
     1TMO -- RUN ABORTED.')
C--   SPOTMO COMPUTES SPOT MOTION COMPONENTS.
C     INPUT REQUIREMENTS:
C     *     NFWD -- NUMBER OF TIME-STEPS FORWARD TO ADVANCE.
C     *     ISEEDT -- RANDOM NUMBER SEED FOR TRACKING
C     *     ISEEDS -- RANDOM NUMBER SEED FOR SCINTILLATION
C     *     OUTPUT -- ARRAY OF OUTPUT SPOT MOTION COMPONENTS
C           OUTPUT(1,1) = OUTPUT(AZ,TR) = AZIM ERROR FROM TRACKING PROCESS
C           OUTPUT(2,1) = OUTPUT(EL,TR)
C           OUTPUT(1,2) = OUTPUT(AZ,SC)
C           OUTPUT(2,2) = OUTPUT(EL,SC)
C           OUTPUT(1,3) = OUTPUT(AZ,NET) = SUM OF TRACK & SCINTILLATION
C           OUTPUT(2,3) = OUTPUT(EL,NET)
C
C--   CHECK ADVANCE
      IF (NFWD.GT.0)   GO TO 300
      WRITE (6,1001) NFWD
      STOP
  300 CONTINUE
C
C--   CHECK FOR TRACKING
C
      IF (ITRACK.EQ.1)   GO TO 350
      OUTPUT(AZ,TR) = 0.
      OUTPUT(EL,TR) = 0.
      GO TO 400
  350 CONTINUE
      DO 380 K=1,NFWD
C--   BACKSPACE NOISE ARRAYS AND GENERATE NEW NOISE
      DO 370 I = AZ, EL
      DO 360 J=1,2
      JJ = 4-J
      XT(I,JJ) = XT(I,JJ-1)
  360 ZT(I,JJ) = ZT(I,JJ-1)
      CALL NORMXX (TMIN   , TMAX   , 0., SDNT, ZT(I,1), ISEEDT)
  370 XT(I,1) = A0*(ZT(I,1)+ZT(I,3)) + A1*ZT(I,2)-B1*XT(I,2)- B2*XT(I,3)
  380 CONTINUE
      OUTPUT(AZ,TR) = XT(AZ,1)*SIGMA(AZ,TR)
      OUTPUT(EL,TR) = XT(EL,1)*SIGMA(EL,TR)
  400 CONTINUE
C
C--   CHECK FOR SCINTILLATION
C
      IF (ISCINT.EQ.1)   GO TO 450
      OUTPUT(AZ,SC) = 0.
      OUTPUT(EL,SC) = 0.
      GO TO 500
  450 CONTINUE
      DO 480 K=1,NFWD
```

```
C--  BACKSPACE NOISE ARRAYS AND GENERATE NEW NOISE
      DO 470 I= AZ, EL
      XS(I,2) = XS(I,1)
      ZS(I,2) = ZS(I,1)
      CALL NORMXX (SMIN   , SMAX   , 0., SDNS, ZS(I,1), ISEEDS)
  470 XS(I,I) = AA0*(ZS(I,I)+ZS(I,2)) - BB*XS(I,2)
  480 CONTINUE
      OUTPUT(AZ,SC) = XS(AZ,I)*SIGMA(AZ,SC)
      OUTPUT(EL,SC) = XS(EL,1)*SIGMA(EL,SC)
  500 CONTINUE
C
C--  DEFINE NET SPOT MOTION
C
      OUTPUT(AZ,NET) = OUTPUT(AZ,TR) + OUTPUT(AZ,SC)
      OUTPUT(EL,NET) = OUTPUT(EL,TR) + OUTPUT(EL,SC)
      RETURN
      END
C>>>>>>>>>>>>>>>>>>>>>>>>>>>>  NORMXX  <<<<<<<<<<<<<<<<<<<<<<<<<<<<<<<<
C--  NORMXX  --  NORMXX  --  NORMXX  --  NORMXX  --  NORMXX  --  NORMXX 00249000
      SUBROUTINE NORMXX (AMIN, AMAX, AMEAN, SIGMA, X, ISEED)            00249100
C                                                                       00249200
C     THIS SUBROUTINE GENERATES A NORMAL DEVIATE                        00249300
C                                                                       00249400
      CALL RANDMM(ISEED,X)                                              00249500
      Z = X                                                             00249600
      CALL RANDMM(ISEED,X)                                              00249700
      X = (((-2.0*ALOG(Z))**0.5)*(COS(6.283*X)))*SIGMA + AMEAN          00249800
      IF (X.LT.AMIN) X = AMIN                                           00249900
      IF (X.GT.AMAX)  X = AMAX                                          00250000
      RETURN                                                            00250100
      END                                                               00250200
C>>>>>>>>>>>>>>>>>>>>>>>>>>>  RANDMM  <<<<<<<<<<<<<<<<<<<<<<<<<<<<<<<<
C--  RANDMM  --  RANDMM  --  RANDMM  --  RANDMM  --  RANDMM  --  RANDMM 00250300
      SUBROUTINE RANDMM(ISEED,X)                                        00250400
C                                                                       00250500
C     THIS SUBROUTINE GENERATES UNIFORM DEVIATES                        00250600
C                                                                       00250700
      ISEED = ISEED*65539                                               00250800
      IF(ISEED)2266,2266,2277                                           00250900
 2266 ISEED = ISEED + 2147483647 + I                                    00251000
 2277 X = ISEED                                                         00251100
      X = X*.4656613E-9                                                 00251200
      RETURN                                                            00251300
      END                                                               00251400
```

APPENDIX B
PROGRAM TO EVALUATE THE AUTOSPECTRUM OF TIME-SAMPLED FIRST-ORDER PROCESSES

Purpose

This is a utility program which evaluates squared modulii associated with time-sampled first-order analog and digital stochastic processes. The phase of the time-sampled digital process is also calculated. Outputs are calculated for a prescribed set of input frequencies.

Description

The squared modulus of a time-sampled, digitally-generated, first-order stochastic process is calculated by means of equations (5.10), (5.12), (5.21a), and (5.21b). The infinite series is truncated at n^*, as in (5.10). The value of n^* is determined implicitly by requiring that the largest relative error of the real and imaginary components of the n^* term in the series be smaller than a specified (input) relative error.

For comparison, the autospectrum of an unsampled analog process having the same specified corner frequency is also calculated and printed. Additionally, the squared modulus of the non-subsampled digital implementation is calculated and printed. The latter derives from the $F(j\omega)$ term in equation (5.10). The phase angle, ϕ, of the time-sampled digital process is calculated from

$$\phi = \tan^{-1}[\mathrm{Im}\{F^*(j\omega)\}/\mathrm{Re}\{F^*(j\omega)\}].$$

Input

The program requires: (a) a descriptive alphameric title card; (b) the desired process standard deviation (used in calculating the analog autospectrum); (c) the sampling time interval; (d) corner frequency; (e) a maximum relative error in the subsampled digital squared modulus; (f) the number of frequencies for which results are to be calculated; (g) the order of subsampling or ratio of sampling interval to digital generation interval; and (h) the array of discrete frequencies for which results are to be calculated.

Output

Examples of program output are shown following the source program listing. Output titles are generally self-descriptive. The input data are immediately echoed. For clarification note that SQ MODUL 0 refers to the squared modulus of the non-subsampled digital process. Except for truncation error, the results of SQ MODUL 0 are identical to SQ MODULUS whenever the subsampling order is unity.

```
      $JOB            RDH,KP=29,RUN=FREE,LINES=58
      C ---------------------------EVAL OF SAMPLED TRANSFER FUNCTION ----------------
      C**** PROGRAM TO EVALUATE THE CHARACTERISTICS OF A
      C**** TIME-SAMPLED FIRST-ORDER DIGITAL DYNAMIC PROCESS.
      C**** INPUTS:
      C**** TITLE = AN ALPHAMERIC DESCRIPTION OF THE FUNCTION
      C**** STDV = STANDARD DEVIATION OF THE DIGITAL PROCESS BEFORE SAMPLING
      C**** T = SAMPLING PERIOD (INTERVAL)
      C**** FS = CORNER FREQUENCY
      C**** EPS = MAX RELATIVE ERROR IN THE SQUARED MODULUS
      C**** MMX = THE NUMBER OF ENTRIES IN THE FREQUENCY ARRAY
      C**** MULTIP = THE ORDER NUMBER OF SUBSAMPLING
      C****          = 1, 2, 3, ETC.
      C**** FREQ(M) = THE ARRAY OF DISCRETE FREQUENCIES AT WICH THE
      C****             TRANSFER FUNCTION IS TO BE EVALUATED.
      C**** THE ORIGINAL  (ANALOG) SQUARED MODULUS IS ALSO CALCULATED.
      C**** TGEN = SAMPLING GENERATION INTERVAL FOR THE DIGITAL PROCESS; TGEN=T/MULTIP
 1          DIMENSION FREQ(50),TITLE(20)
 2          DATA TWOPI/6.283185/
 3       11 CONTINUE
 4          READ (5,100,END=1) TITLE
 5      100 FORMAT(20A4)
 6          WRITE (6,200) TITLE
 7      200 FORMAT(1H1,20A4)
 8          READ (5,300) STDV,T,FS,EPS,MMX,MULTIP
 9      300 FORMAT(4F10.0,2I3)
10          WRITE (6,400) STDV,T,FS,EPS,MMX,MULTIP
11      400 FORMAT(1H0,6X,4HSTDV,9X,1HT,8X,2HFS,7X,3HEPS,2X,8HMX FREQS,
           1 10H ORD S SMP/1H ,3F10.4,F10.6,7X,I3,7X,I3)
12          READ (5,500) (FREQ(I),I=1,MMX)
13      500 FORMAT(8F10.0)
      C**** WRITE HEADINGS
14          WRITE (6,600)
15      600 FORMAT(1H0,6X,9HFREQ (HZ),3X,12HANAL AUTOSPK,5X,10HSQ MODUL 0,
           1 5X,10HSQ MODULUS,8X,7HMODULUS,6X,9HPHASE (D))
16          OMEGS=TWOPI*FS
      C**** COMPUTE THE CONSTANTS FOR THE DIGITAL TRANSFER FUNCTION
17          TGEN=T/FLOAT(MULTIP)
18          PI=TWOPI/2.
19          AF=ATAN(PI*FS*TGEN)
20          AO=AF/(AF+1.)
21          B=(AF-1.)/(AF+1.)
22          CONREL=AO*(1.+B)
23          CONIMG=-AO*(1.-B)
24          CONC=2.*B
25          COND=1.+B**2
26          GAIN=SQRT(2.*TGEN/AO)*STDV
      C**** START FREQUENCY LOOP
27          DO 10 M=1,MMX
28          F=FREQ(M)
29          OMEG=TWOPI*F
30          COSX=COS(OMEG*TGEN)
31          SINX=SIN(OMEG*TGEN)
32          IPASS=0
      C**** COMPUTE THE REAL PART OF THE TRANSFER FUNCTION
33          DENOM=COND+CONC*COSX
34          SUMREL=CONREL*(1.+COSX)/DENOM
35          SAVE1=SUMREL
```

```
36          SUMIMG=CONIMG*SINX/DENOM
37          SAVE2=SUMIMG
      C**** ACCUMULATE OVER POSITIVE AND NEGATIVE HARMONICS
38          DO 20 N=1,24
39          ISWPOS=0
40          ISWNEG=0
41          OMEGN=TWOPI*FLOAT(N)/T
42          TERMP=0.
43          TERMN=0.
44          OMEGPT=(OMEG+OMEGN)*TGEN
45          OMEGMT=(OMEG-OMEGN)*TGEN
46          IF(OMEGPT.GT.PI) ISWPOS=1
47          IF(OMEGMT.LT.-PI.OR.OMEGMT.GT.PI) ISWNEG=1
48          IF(ISWPOS.EQ.1) GO TO 30
49          COSP=COS(OMEGPT)
50          DENOMP=COND+CONC*COSP
51          TERMP=CONREL*(1.+COSP)/DENOMP
52       30 CONTINUE
53          IF(ISWNEG.EQ.1) GO TO 35
54          COSN=COS(OMEGMT)
55          DENOMN=COND+CONC*COSN
56          TERMN=CONREL*(1.+COSN)/DENOMN
57       35 CONTINUE
58          R=TERMP+TERMN
59          SUMREL=SUMREL+R
60          IF(R/SUMREL.LT.EPS.AND.N.GT.4) IPASS=1
      C**** COMPUTE THE NEGATIVE OF THE IMAGINARY PART OF THE TRANSFER FUNCTION
61          TERMP=0.
62          TERMN=0.
63          IF(ISWPOS.EQ.1) GO TO 40
64          TERMP=CONIMG*SIN(OMEGPT)/DENOMP
65       40 CONTINUE
66          IF(ISWNEG.EQ.1) GO TO 45
67          TERMN=CONIMG*SIN(OMEGMT)/DENOMN
68       45 CONTINUE
69          R=TERMP+TERMN
70          SUMIMG=SUMIMG+R
71          IF(ABS(TERMP).LT.EPS.AND.ABS(TERMN).LT.EPS.AND.IPASS.EQ.1) GO TO
           1 25
72       20 CONTINUE
73       25 CONTINUE
      C**** COMPUTE THE SQUARED MODULUS OF THE CORRESPONDING ANALOG
74          AGAN=SQRT(2./PI/FS)*STDV
75          AMODSQ=AGAN**2/(1.+(OMEG/OMEGS)**2)
      C**** COMPUTE THE SQUARED MODULUS AND PHASE
76          SQMODO=(SAVE1**2+SAVE2**2)*GAIN**2
77          SQMOD=(SUMREL**2+SUMIMG**2)*GAIN**2
78          PHASE=57.3*ATAN2(-SUMIMG,SUMREL)
79          FMOD=SQRT(SQMOD)
      C**** WRITE FREQUENCY,SQUARED MODULUS,MODULUS,AND PHASE
80          WRITE (6,120) F,AMODSQ,SQMODO,SQMOD,FMOD,PHASE
81       120 FORMAT(1H ,F15.5,4E15.5,F15.2)
82        10 CONTINUE
83          GO TO 11
84         1 CONTINUE
85          CALL EXIT
86          STOP
87          END
```

TIME-SAMPLED FIRST-ORDER DYNAMIC SYSTEM AT SAMP. RATE 10 HZ

STDV	T	FS	EPS	MX FREQS	ORD S	SMP
0.1650	0.1000	3.0000	0.000001	20	2	

FREQ (HZ)	ANAL AUTOSPK	SQ MODUL 0	SQ MODULUS	MODULUS	PHASE (D)
0.01000	0.57773E-02	0.89046E-02	0.89046E-02	0.94364E-01	0.16
0.05000	0.57757E-02	0.89019E-02	0.89011E-02	0.94346E-01	0.82
0.10000	0.57709E-02	0.88934E-02	0.88903E-02	0.94288E-01	1.65
0.20000	0.57518E-02	0.88596E-02	0.88472E-02	0.94060E-01	3.29
0.30000	0.57201E-02	0.88038E-02	0.87761E-02	0.93681E-01	4.92
0.40000	0.56764E-02	0.87266E-02	0.86778E-02	0.93155E-01	6.53
0.50000	0.56212E-02	0.86291E-02	0.85537E-02	0.92486E-01	8.13
0.60000	0.55551E-02	0.85125E-02	0.84055E-02	0.91681E-01	9.70
0.70000	0.54790E-02	0.83782E-02	0.82349E-02	0.90746E-01	11.24
0.80000	0.53938E-02	0.82276E-02	0.80441E-02	0.89689E-01	12.74
1.00000	0.51996E-02	0.78848E-02	0.76106E-02	0.87239E-01	15.63
1.20000	0.49804E-02	0.74978E-02	0.71234E-02	0.84400E-01	18.33
1.50000	0.46219E-02	0.68645E-02	0.63322E-02	0.79575E-01	21.99
2.00000	0.39997E-02	0.57659E-02	0.49829E-02	0.70589E-01	26.82
2.50000	0.34096E-02	0.47247E-02	0.37467E-02	0.61210E-01	29.82
3.00000	0.28887E-02	0.38075E-02	0.27172E-02	0.52126E-01	30.59
3.50000	0.24469E-02	0.30325E-02	0.19257E-02	0.43883E-01	28.57
4.00000	0.20798E-02	0.23925E-02	0.13725E-02	0.37047E-01	22.94
4.50000	0.17776E-02	0.18702E-02	0.10470E-02	0.32358E-01	13.12
5.00000	0.15293E-02	0.14464E-02	0.93975E-03	0.30655E-01	0.00

TIME-SAMPLED FIRST-ORDER DYNAMIC SYSTEM AT SAMP. RATE 20 HZ

STDV	T	FS	EPS	MX FREQS	ORD S	SMP
0.1650	0.0500	3.0000	0.000001	24		1

FREQ (HZ)	ANAL AUTOSPK	SQ MODUL 0	SQ MODULUS	MODULUS	PHASE (D)
0.01000	0.57773E-02	0.89046E-02	0.89046E-02	0.94364E-01	0.20
0.05000	0.57757E-02	0.89019E-02	0.89019E-02	0.94350E-01	1.02
0.10000	0.57709E-02	0.88934E-02	0.88934E-02	0.94305E-01	2.04
0.20000	0.57518E-02	0.88596E-02	0.88596E-02	0.94125E-01	4.08
0.30000	0.57201E-02	0.88038E-02	0.88038E-02	0.93828E-01	6.11
0.40000	0.56764E-02	0.87266E-02	0.87266E-02	0.93416E-01	8.13
0.50000	0.56212E-02	0.86291E-02	0.86291E-02	0.92893E-01	10.13
0.60000	0.55551E-02	0.85125E-02	0.85125E-02	0.92263E-01	12.12
0.70000	0.54790E-02	0.83782E-02	0.83782E-02	0.91532E-01	14.07
0.80000	0.53938E-02	0.82276E-02	0.82276E-02	0.90706E-01	16.01
1.00000	0.51996E-02	0.78848E-02	0.78848E-02	0.88796E-01	19.78
1.20000	0.49804E-02	0.74978E-02	0.74978E-02	0.86590E-01	23.42
1.50000	0.46219E-02	0.68645E-02	0.68645E-02	0.82852E-01	28.60
2.00000	0.39997E-02	0.57659E-02	0.57659E-02	0.75933E-01	36.42
2.50000	0.34096E-02	0.47247E-02	0.47247E-02	0.68736E-01	43.25
3.00000	0.28887E-02	0.38075E-02	0.38075E-02	0.61705E-01	49.17
3.50000	0.24469E-02	0.30325E-02	0.30325E-02	0.55069E-01	54.30
4.00000	0.20798E-02	0.23925E-02	0.23925E-02	0.48913E-01	58.78
4.50000	0.17776E-02	0.18702E-02	0.18702E-02	0.43246E-01	62.73
5.00000	0.15293E-02	0.14464E-02	0.14464E-02	0.38031E-01	66.24
6.00000	0.11555E-02	0.82692E-03	0.82692E-03	0.28756E-01	72.26
7.00000	0.89648E-03	0.42684E-03	0.42684E-03	0.20660E-01	77.36
8.00000	0.71227E-03	0.17866E-03	0.17866E-03	0.13366E-01	81.86
10.00000	0.47703E-03	0.17047E-15	0.11898E-17	0.10908E-08	0.00

Next page is blank.

APPENDIX C
PROGRAM TO EVALUATE THE AUTOSPECTRUM OF SECOND-ORDER STOCHASTIC PROCESSES

Purpose

This utility program calculates and prints spectral results for analog and digital implementations of a general, second-order stochastic process. The x-process is specified in terms of its standard deviation, sampling generation interval (for the digital implementation), corner frequency, and damping ratio. Analog and digital squared modulii are calculated for the specified process and a digital squared modulus is calculated for a Butterworth process having the specified corner frequency. A digital autospectrum is calculated for the specified process and an analog autospectrum is calculated for the corresponding Butterworth process.

Description

The analog squared modulus is developed from equation (5.40). The digital squared modulus uses (5.35) with the coefficients (a's and b's) developed from the following generalization of equation (4.6):

$$D = \omega_a^2 + 2\zeta\omega_a + 1$$

$$b_2 = (\omega_a^2 - 2\zeta\omega_a + 1)/D,$$

where ζ is the damping ratio. The digital noise autospectrum, Γ_{nn}, used in calculating the x-process autospectrum, Γ_{xx}, via (5.38) is obtained from (5.39). Note that the ratio of variances $\gamma_{xx}(0)/\gamma_{nn}(0)$ in (4.15a) is a general result and holds for any set of the (a, b) coefficients, providing, of course, that the denominator in (4.15a) is positive. The squared modulus of the second-order digital Butterworth process is evaluated using equations (5.36) and (5.37). The analog Butterworth autospectrum uses equations (1.1) and (1.5).

Input

The program requires: (a) a descriptive alphameric title card; (b) the process standard deviation desired (in arbitrary units); (c) the sampling generation time interval (arbitrary units); (d) the crossover frequency (compatible units); (e) the damping ratio; (f) the number of frequencies at which the spectra are to be evaluated; and (g) an array of frequencies at which the spectra are to be evaluated (compatible units).

Output

An example of program output is shown following the source program listing. Output names are defined below:

A.GAIN	the gain constant in the analog autospectrum
D.GAIN	the gain constant (noise autospectum) in the digital autospectrum
FREQ	frequency
ANL.SQ.MOD	analog squared modulus
DIG.SQ.MOD	Butterworth digital squared modulus
H22	squared modulus of the specified digital process
ANL.SPK	analog autospectrum
DIG.SPK	digital autospectrum

```
      $JOB            RDH,KP=29,RUN=FREE,LINES=58
      C**** PROGRAM TO EVALUATE THE AUTOSPECTRUM OF SECOND-ORDER
      C**** STOCHASTIC PROCESSES.
      C****
      C**** INPUTS:
      C**** TITLE = DESCRIPTIVE ALPHAMERIC TITLE
      C**** STDVX = THE PROCESS STANDARD DEVIATION
      C**** T = SAMPLING GENERATION TIME INTERVAL
      C**** FA = ANALOG CORNER FREQUENCY
      C**** DAMP = DAMPING RATIO
      C**** MMX = NUMBER OF ENTRIES IN THE FREQUENCY ARRAY
      C**** FREQ(M) = THE ARRAY OF DISCRETE FREQUENCIES AT WHICH THE
      C****             TRANSFER FUNCTIONS ARE TO BE EVALUATED.
      C****
      C**** THE ANALOG SQUARED MODULUS IS ALSO CALCULATED.
 1          IMPLICIT REAL*8(A-H,O-Z)
 2          DIMENSION FREQ(50),TITLE(20)
 3          DATA TWOPI/6.283185D0/
 4          RT2=DSQRT(2.0D0)
 5       11 CONTINUE
 6          READ (5,100,END=1) TITLE
 7      100 FORMAT(20A4)
 8          WRITE (6,200) TITLE
 9      200 FORMAT(1H1,20A4)
10          READ (5,300) STDVX,T,FA,DAMP,MMX
11      300 FORMAT(4F10.0,I3)
12          WRITE (6,400) STDVX,T,FA,DAMP,MMX
13      400 FORMAT(1H0,4X,6HSTDV.X,9X,1HT,8X,2HFA,6X,4HDAMP,2X,8HMX FREQS/
           1 1H ,4F10.5,7X,I3)
      C**** READ IN FREQUENCIES
14          READ (5,500) (FREQ(I),I=1,MMX)
15      500 FORMAT(8F10.0)
16          PI=TWOPI/2.
17          WA=DTAN(PI*FA*T)
      C**** GENERATE RHO--THE RATIO OF PROCESS TO NOISE VARIANCE
18          D=WA**2+2.*DAMP*WA+1.
19          A0=WA**2/D
20          A1=2.*A0
21          A2=A0
22          B1=2.*(WA**2-1.)/D
23          B2=(WA**2-2.*DAMP*WA+1.)/D
24          AA1=B1
25          AA2=1.-B1**2-B2**2
26          BB1=1.+B2
27          BB2=-2.*B1*B2
28          CC1=A0*A1+A2*(A1-B1*A0)
29          CC2=-2.*A0*A1*B1-2.*A0*A2*B2-2.*A2*B1*(A1-B1*A0)+A0**2+A1**2+A2**2
30          RHO=(CC1*BB2-BB1*CC2)/(AA1*BB2-BB1*AA2)
      C**** GENERATE THE NOISE DENSITY
31          GAMN=2.*T*STDVX**2/RHO
      C**** GENERATE THE ANALOG GAIN
32          AGAIN=2.*RT2*STDVX**2/PI/FA
      C**** WRITE GAIN CONSTANTS
33          WRITE (6,600) AGAIN,GAMN
34      600 FORMAT(1H0,4X,6HA.GAIN,4X,6HD.GAIN/1H ,2F10.5)
      C**** DEVELOP COEFFICIENTS FOR THE DIGITAL BUTTERWORTH MODULUS
35          C1=WA**4
36          C2=3.*(C1+1.)
```

```
      C3=4.*(C1-1.)
      C4=C1+1.
      ARG1=TWOPI*T
      ARG2=2.*ARG1
      WRITE (6,800)
C**** START FREQUENCY LOOP
      DO 10 M=1,MMX
      F=FREQ(M)
      COS1=DCOS(F*ARG1)
      SIN1=DSIN(F*ARG1)
      COS2=DCOS(F*ARG2)
      SIN2=DSIN(F*ARG2)
      FR=F/FA
      ANLMDS=1./((1.-FR**2)**2+4.*DAMP**2*FR**2)
      SPKA=ANLMDS*AGAIN
      H22=((A0+A1*COS1+A2*COS2)**2+(A1*SIN1+A2*SIN2)**2)/
     1 ((1.+B1*COS1+B2*COS2)**2+(B1*SIN1+B2*SIN2)**2)
      DIGMDS=H22
      SPKD=DIGMDS*GAMN
      DIGMDS=C1*(3.+4.*COS1+COS2)/(C2+C3*COS1+C4*COS2)
C**** WRITE OUTPUT
      WRITE (6,700) F,ANLMDS,DIGMDS,H22,SPKA,SPKD
  700 FORMAT(1H ,4F12.5,2D12.5)
  800 FORMAT(1H0,8X,4HFREQ,12H  ANL.SQ.MOD,12H  DIG.SQ.MOD,9X,3HH22,5X,
     1 7HANL.SPK,5X,7HDIG.SPK)
   10 CONTINUE
      GO TO 11
    1 CALL EXIT
      END
```

SAMPLE OF SECOND ORDER SPECTRUM WITH CORNER FREQ = 0.7 HZ AND DAMP = 0.1

STDV.X	T	FA	DAMP	MX FREQS
1.00000	0.05000	0.70000	0.10000	24

A.GAIN	D.GAIN
1.28617	0.18332

FREQ	ANL.SQ.MOD	DIG.SQ.MOD	H22	ANL.SPK	DIG.SPK
0.01000	1.00040	1.00000	1.00040	0.12867D 01	0.18339D 00
0.05000	1.01007	0.99997	1.00999	0.12991D 01	0.18515D 00
0.10000	1.04121	0.99959	1.04088	0.13392D 01	0.19081D 00
0.20000	1.18111	0.99348	1.17959	0.15191D 01	0.21624D 00
0.30000	1.48426	0.96778	1.48003	0.19090D 01	0.27132D 00
0.40000	2.14306	0.90460	2.13245	0.27563D 01	0.39092D 00
0.50000	3.84160	0.79475	3.81375	0.49409D 01	0.69913D 00
0.60000	10.02254	0.65042	9.94517	0.12891D 02	0.18231D 01
0.70000	25.00000	0.50000	25.00000	0.32154D 02	0.45830D 01
0.80000	6.85139	0.36840	6.75289	0.88120D 01	0.12379D 01
1.00000	0.85842	0.19098	0.83193	0.11041D 01	0.15251D 00
1.20000	0.25797	0.10087	0.24619	0.33179D 00	0.45130D-01
1.50000	0.07642	0.04280	0.07095	0.98293D-01	0.13007D-01
2.00000	0.01937	0.01315	0.01694	0.24907D-01	0.31045D-02
2.50000	0.00721	0.00502	0.00583	0.92735D-02	0.10685D-02
3.00000	0.00331	0.00220	0.00242	0.42538D-02	0.44392D-03
3.50000	0.00173	0.00105	0.00112	0.22291D-02	0.20601D-03
4.00000	0.00100	0.00053	0.00056	0.12820D-02	0.10231D-03
4.50000	0.00061	0.00028	0.00029	0.79009D-03	0.52898D-04
5.00000	0.00040	0.00015	0.00015	0.51363D-03	0.27895D-04
6.00000	0.00019	0.00004	0.00004	0.24476D-03	0.76848D-05
7.00000	0.00010	0.00001	0.00001	0.13117D-03	0.18470D-05
8.00000	0.00006	0.00000	0.00000	0.76537D-04	0.30430D-06
10.00000	0.00002	0.00000	0.00000	0.31180D-04	0.94423D-33

SAMPLE OF SECOND ORDER SPECTRUM WITH CORNER FREQ = 0.7 HZ AND DAMP = 0.7

STDV.X	T	FA	DAMP	MX FREQS
1.00000	0.05000	0.70000	0.70000	24

A.GAIN	D.GAIN
1.28617	1.28149

FREQ	ANL.SQ.MOD	DIG.SQ.MOD	H22	ANL.SPK	DIG.SPK
0.01000	1.00001	1.00000	1.00001	0.12862D 01	0.12815D 01
0.05000	1.00018	0.99997	1.00018	0.12864D 01	0.12817D 01
0.10000	1.00040	0.99959	1.00040	0.12867D 01	0.12820D 01
0.20000	0.99661	0.99348	0.99669	0.12818D 01	0.12772D 01
0.30000	0.97429	0.96778	0.97466	0.12531D 01	0.12490D 01
0.40000	0.91444	0.90460	0.91535	0.11761D 01	0.11730D 01
0.50000	0.80652	0.79475	0.80780	0.10373D 01	0.10352D 01
0.60000	0.66208	0.65042	0.66307	0.85155D 00	0.84972D 00
0.70000	0.51020	0.50000	0.51020	0.65621D 00	0.65382D 00
0.80000	0.37683	0.36840	0.37565	0.48467D 00	0.48139D 00
1.00000	0.19672	0.19098	0.19404	0.25302D 00	0.24866D 00
1.20000	0.10505	0.10087	0.10210	0.13512D 00	0.13084D 00
1.50000	0.04566	0.04280	0.04315	0.58726D-01	0.55300D-01
2.00000	0.01486	0.01315	0.01321	0.19107D-01	0.16933D-01
2.50000	0.00613	0.00502	0.00504	0.78818D-02	0.64529D-02
3.00000	0.00296	0.00220	0.00220	0.38095D-02	0.28236D-02
3.50000	0.00160	0.00105	0.00105	0.20579D-02	0.13503D-02
4.00000	0.00094	0.00053	0.00053	0.12066D-02	0.68349D-03
4.50000	0.00059	0.00028	0.00028	0.75336D-03	0.35792D-03
5.00000	0.00038	0.00015	0.00015	0.49429D-03	0.19044D-03
6.00000	0.00019	0.00004	0.00004	0.23836D-03	0.53057D-04
7.00000	0.00010	0.00001	0.00001	0.12866D-03	0.12833D-04
8.00000	0.00006	0.00000	0.00000	0.75411D-04	0.21219D-05
10.00000	0.00002	0.00000	0.00000	0.30886D-04	0.66629D-32

DISTRIBUTION LIST

No. of Copies	
1	Department of Defense Office of the Defense Director, Research & Engineering ATTN: Assistant Director (Test Resources) Room 3D 116, The Pentagon Washington, DC 20301
	HQ, Department of the Army
1	ATTN: DAMO-RDQ
1	DAMA-CSM-CM
	Washington, DC 20310
	Commander US Army Materiel Development & Readiness Command
1	ATTN: DRCDE-R
1	DRCBSI-F
	5001 Eisenhower Avenue Alexandria, VA 22333
	Commander US Army Armament Materiel Readiness Command
1	ATTN: DRSAR-EN
1	DRSAR-LE
2	DRSAR-SA
6	DRSAR-SAM
1	DRSAR-PA
1	DRSAR-AS
	Rock Island, IL 61201
	Commander US Army Armament Research & Development Command
2	ATTN: DRDAR-SEA
1	DRDAR-SCF
	Dover, NJ 07801
	Commander US Army Test and Evaluation Command
1	ATTN: DRSTE-SY
1	DRSTE-TA
1	DRSTE-ME
	Aberdeen Proving Ground, MD 21005
1	Office of the Project Manager of Army Tactical Data Systems ATTN: DRCPM-TDF-TF Ft. Monmouth, NJ 07703

No. of Copies

Commander
US Army Electronics Command
1 ATTN: DRSEL-SA
2 DRSEL-RD
1 DRSEL-CT-L-A
Fort Monmouth, NJ 07703

Commander
US Army Missile Research and Development Command
1 ATTN: DRDMI-CM
1 DRDMI-D
1 DRDMI-RGN
2 DRDMI-CAWS-FO
1 DRDMI-RGT
1 DRCPM-LD
Redstone Arsenal, AL 35809

1 Project Manager for M110E2
ATTN: DRCPM-M110E2
Rock Island, IL 61201

Project Manager for Cannon Artillery Weapons Systems
1 ATTN: DRCPM-CAWS-SI
2 DRCPM-CAWS-GP

Dover, NJ 07801

1 Product Manager for Advanced Attack Helicopter Systems
US Army Aviation Systems Command
St. Louis, MO 63166

1 Project Manager for AH-1 Cobra Series Aricraft
US Army Materiel Development & Readiness Command
P.O. Box 209
St. Louis, MO 63166

Commander
US Army Materiel Systems Analysis Activity
1 ATTN: DRXSY-GS
1 DRXSY-C
1 DRXSY-T
1 DRXSY-D
1 DRXSY-AAM
1 DRXSY-DS
Aberdeen Proving Ground, MD 21005

No. of Copies

Commander
US Army Tank Automotive Materiel and Readiness Command
1 ATTN: DRSTA-S
1 DRSTA-R
1 DRSTA-V
Warren, MI 48090

Commander
HQ, US Army Aviation Systems Command
1 ATTN: DRSAV-E
1 DRSAV-W
1 DRSAV-D
1 DRSAV-WR
P.O. Box 209, Main Office
St. Louis, MO 63166

Commander
Rock Island Arsenal
2 ATTN: DRDAR-LCA-PP
2 SARRI-ADL
Rock Island, IL 61201

1 Commander
Watervliet Arsenal
ATTN: SARWV-RD
Watervliet, NY 12189

Commander
Picatinny Arsenal
1 ATTN: SARPA-PA
1 SARPA-AD
1 SARPA-ND
1 SARPA-TS
Dover, NJ 07801

Commander/Director
US Army Armament Research & Development Command
1 ATTN: DRDAR-CLY-A
1 DRDAR-CLJ-I
2 DRDAR-BLB
Aberdeen Proving Ground, MD 21010

1 Project Manager for Selected Ammunition
US Army Materiel Development & Readiness Command
ATTN: DRCPM-SA2
Dover, NJ 07801

DISTRIBUTION LIST (Cont)

No. of Copies

	Commander US Army Ballistic Research Laboratories
1	ATTN: DRXBR-EB
1	DRXBR-TB
1	DRXBR-VL
	Aberdeen Proving Ground, MD 21005
1	Commander Army Ordnance Center & School ATTN: ATSL-CTD-MF Aberdeen Proving Ground, MD 21005
3	Commander Human Engineering Laboratories ATTN: DRXHE-SP Aberdeen Proving Ground, MD 21005
1	Commander US Army Aberdeen Research & Development Center ATTN: STEAP-TL Aberdeen Proving Ground, MD 21005
1	Office of Project Manager-Smoke Obscurants ATTN: DRCPM-SMK-T Aberdeen Proving Ground, MD 21005
1	Commander US Army Armor School Fort Knox, KY 40121
	Commander US Army Field Artillery Board
1	ATTN: ATZR-BD
1	ATZR-BDAS
	Ft. Sill, OK 73503
	Commandant US Army Field Artillery School
1	ATTN: ATSF-CD-R
1	ATSF-CA-RA (TCAD)
1	ATSF-WD
1	ATSF-CD
	Fort Sill, OK 73503

DISTRIBUTION LIST (Cont)

No. of Copies	
1	Commandant US Army Infantry School Fort Benning, GA 31905
1	Commander US Army Missile & Munitions Center & School Redstone Arsenal, AL 35809
1	Commander Modern Army Selected System Test, Evaluation & Review Fort Hood, TX 76544
1	Commander US Army Combat Developments Experimentation Command Fort Ord, CA 93941
1	Commander US Army TRADOC Systems Analysis Activity White Sands Missile Range White Sands, NM 88002
2	Commander Harry Diamond Laboratories ATTN: DMXDO-PP Washington, DC 24038
1	Director Advanced Research Projects Agency 1400 Wilson Boulevard Arlington, VA 22209
1	Commander US Army Concepts Analysis Agency 8120 Woodmont Avenue Bethesda, MD 20014
1	Commander Combat Systems Group ATTN: CDMSD-M Fort Leavenworth, KS 66027
1	Commander USA Combined Arms Combat Developments Activity ATTN: ATCACC Fort Leavenworth, KS 66027

DISTRIBUTION LIST (Cont)

No. of Copies	
1	Commander Defense Logistics Studies Information Exchange Fort Lee, VA 23801
	Commander US Army Mobility Equipment Research & Development Center
1	ATTN: STSFB-B
1	STSFB-ZN
	Fort Belvoir, VA 22060
1	Commander US Army Armor Training Center ATTN: AMSTB-CO-MM Fort Knox, KY 40121
2	Commander US Naval Weapons Laboratory Code GS, Mr. Godius Dahlgren, VA 22448
	Chief, Naval Operations
1	ATTN: OP 96
1	OP 982F
	Washington, DC 00350
1	Commander Naval Weapons Center Code 4072 Mr. E. Breitenstein China Lake, CA 93555
	Commander US Army White Sands Missile Range
1	ATTN: STEWS-TE-MD
1	STEWS-TE-PC
	White Sands Missile Range, NM 88002
1	Chief, Naval Materiel ATTN: MAT 0362 Washington, DC 20360
1	Director US Marine Corps Development and Education Center Quantico, VA 22134

DISTRIBUTION LIST (Cont)

No. of Copies	
1	Atmospheric Science Laboratory ATTN: AMSEL-BL-AS White Sands Missile Range, NM 88002
12	Defense Documentation Center Cameron Station Alexandria, VA 22314

Next page is blank.